Article

Not peer-reviewed version

Understanding Multi-hazard Interaction and Impact on Small Islands Community: Insights from an Active Volcano Island of Ternate, Indonesia

Mohammad Ridwan Lessy *, Jonatan Lassa *, Kerstin K Zander *

Posted Date: 13 June 2024

doi: 10.20944/preprints202406.0868.v1

Keywords: Multi-hazard; compounding hazard; small island communities; Ternate; Indonesia; systemic risk; hydrometeorological and geological hazard

Article

Understanding Multi-Hazard Interaction and Impact on Small Islands Community: Insights from an Active Volcano Island of Ternate, Indonesia

Mohammad Ridwan Lessy [1,2,*], Jonatan Lassa [1,3,*] and Kerstin K. Zander [4]

[1] Humanitarian, Emergency & Disaster Management Studies, Faculty of Arts and Society, Charles Darwin University; Darwin, 0810, Australia; mohammadridwanlessy@cdu.edu.au
[2] Marine Science Department, Universitas Khairun, Ternate 97718, Indonesia
[3] GNZ Science, New Zealand; Jonatan.lassa@cdu.edu.au
[4] The Northern Institute, Charles Darwin University, Darwin, 0810, Australia; kerstin.zander@cdu.edu.au
* Correspondence: mohammadridwanlessy@cdu.edu.au; Tel.: +61401731389; jonatan.lassa@cdu.edu.au Tel.; +61466880630; kerstin.zander@cdu.edu.au

Abstract: Current trends in systemic risk literature provide new insights into multi-hazard risks that interact and compound with built environments, creating more significant impacts on socio-economic and human systems. Recurrent natural hazards and extreme weather events are more likely to compound and cascade into more impactful events, especially in vulnerable societies. In small-island communities (SICS), including large archipelagos and Small Island Developing States (SIDS), the long-term impact of multi-, compounding-, and cascading-hazards (MCC hazards) can result in persistent vulnerability and residual risks. This is due to delayed responses, limited resources, poverty, fewer evacuation options, and inadequate market and infrastructure. Using Ternate, a densely populated small volcanic island in North Maluku, Indonesia, as a case study, this paper assesses the impacts of seven types of natural hazards: flash floods, landslides, extreme weather, extreme waves and abrasion, earthquakes, tsunamis, and volcanic eruptions. The research focuses on the multi-hazard impact on population, land use, and infrastructure exposures in 60 villages in Ternate. The findings highlight population density, land use, and infrastructure exposure to multi-hazard risks, providing valuable information on potential losses in future hazard events.

Keywords: multi-hazard; compounding hazard; small island communities; Ternate; Indonesia; systemic risk; hydrometeorological and geological hazard

1. Introduction

Current trends in disaster studies literature highlight a growing awareness of multi-hazard risks that interact, compound, and cascade, creating more systematic impacts on social, economic, and built-environment systems. These multi-hazard impacts often result in significant losses of human lives, livelihoods, and the built environment [1]. In light of this, the Sendai Framework emphasizes the need for multi-hazard approaches, recognizing that hazardous events can coincide, cascade, or accumulate over time, leading to interrelated effects [2].

Multi-Hazard Risk Assessment (MHRA) is the primary tool for analyzing the consequences of multi-hazard disasters [3]. The objective of MHRA is to comprehensively analyze and chart the anticipated losses from different natural hazards on the social, environmental, and economic assets of a region [4,5].

Imagination from existing disaster and climate change studies suggests several trajectories to systemic risk. Hazard-prone areas susceptible to multiple hazards often experience cascading events, such as the excessive rainfall in northern Pakistan in 2016 that led to devastating flooding and landslides [6–8]. Additionally, large-scale natural hazard events can release energy equivalent to tens of thousands of Hiroshima atomic bombs, causing systemic infrastructure failures and widespread fatalities. A notable example is the 9.0 magnitude earthquake on Boxing Day 2004 in Aceh, which triggered a tsunami affecting over a dozen countries and resulting in nearly 230,000 deaths, including 165,000 in Aceh, Indonesia [9].

Scholars and policymakers have noted a significant increase in literature on multi-hazard risk assessment, impact studies, and systemic risk over the past 20 years [10]. Articles titled "systemic risk" have doubled in the Scopus database, especially since 2020 when COVID-19 began affecting the world [11]. Multi-hazard impacts on small islands are likely to be less widespread but more intense and the long-term effects are more systemic from future climate change. The IPCC Assessment Report 2022 emphasizes the urgency of considering climate change-related natural hazards on small islands [12], which often interact with geological dynamics, leading to cascading effects, as seen in the recent Tonga volcano eruption [13].

It is imperative to build resilience in small island communities (SICs) either in the context of middle-income countries large archipelagos or small-island development states (SIDS).The main attributes responsible for causing compounding vulnerabilities in the small island are settlements isolation, significant rural presence, being close to the sea, limited size, reliance on natural resources, and often, inadequate adaptive capacity, prevalent poverty, income inequality, and poor educational attainment [14,15]. Furthermore, SICs face significant vulnerability and are at risk of food insecurity and enduring poverty because they rely on mainland agriculture and restricted access to market institutions and technologies [16].

A better understanding of the spatial characteristics of multi-hazard risk is crucial for implementing effective, evidence-based policies and programs for disaster risk reduction. We argue that in small-island communities (SICS) settings – either in the context of large archipelagos as well as Small Island Development States (SIDS) - the long-term impact of multi-, compounding-, cascading- hazards (MCC hazards) can be long-lasting and emerging as viscous cycles of vulnerability and residual risks due to the lack of public attention tends delay response and recovery, limited resources and poverty, fewer evacuation options, and lack of market and infrastructure.

One of the key problems in SICs contexts is that there is barely local expert to produce and update cascading and compounding behaviour of multi-hazard aggregation and interaction. Current promotion of systemic risk framework that demands rigorous computing capability to demonstrate compounding and cascading behaviour can be an oxymoron as it can marginalise local experts who have limited access to knowledge, skills, and resources to plan for multi-hazard risk scenarios.

This paper addresses two key questions: (1) How are hazard interactions modelled in a multi-hazard map, and what are their hazard levels? (2) How is the exposure level reflected based on population and infrastructure? It demonstrates the first stage of research on the multi-hazard impact of a SIC, focusing on population, land use, and infrastructure exposures. It also offers insights into how local experts can analyse and visualize results for multi-hazard exposure assessment on Ternate Island, Indonesia.

Using a case study from one of the world's most densely populated small volcanic island communities, Ternate, North Maluku, Indonesia, this paper assesses the impacts of nine types of natural hazards, including flash floods, landslides, extreme weather, extreme waves and abrasion, earthquakes, tsunamis, and volcanic activity. This research by a PhD student from Ternate, identifies the spatial distribution of multiple natural hazards in the small island context (SIC) of Ternate Island, one of the most densely populated small volcano islands in Eastern Indonesia that has been exposed to a dozen of recurrent natural hazards. The population data indicated that Ternate Island has a population increase from 192.2k in 2012 to 194.6k people in 2023 or annual rate at 2.7 annually - with a population density of 2.419/km^2 in 2012 to 2.450 in 2023 [17]. The Island is also experiencing rapid growth of settlement coastal area development at the rate of 1.48% per year [17].

2. Multi-Hazard Mapping: Challenges and Opportunities

2.1. Basic Definition

There is a consensus shared by the United Nations that defines a 'single hazard' of natural or man-made as a process that can result in loss of life, injury or other health consequences, damage to property, loss of livelihoods and services, disruption to social and economic activities, or harm to the environment [18,19]. 'Multi-hazards' and compounding hazard (or compound events) are often used interchangeable to suggests a complex aggregation of hazards involving interactions and or association between multiple events and dangers.

When a society has to deal with more than one parallel hazard at a time in a locality, experts often label such a reality as multi-hazard event [10]. While the Artificial Intelligence such as [20] suggests that 'multi-hazard disaster risk' as 'potential adverse impacts arising from multiple hazards occurring simultaneously or sequentially. The key features include hazard interactions, cumulative impacts, vulnerability and exposure, preparedness, and response as well as resilience building [20].

Multi-hazards can be serial hazards (one hazard built on the impact of previous hazards on a society (see e.g., [21] or parallel hazards (more than one hazard occurs simultaneously) (e.g., [3] and each can also have compounding and cascading impacts. The terms such as multi-hazard, compounding and cascading hazards have many interlinked and overlapping definitions [10]. These interactions might result in a higher impact than expected from individual (parallel) hazards [22]. The reason for this is that multi-dangers have dynamic characteristics, involve several hazards, occur repeatedly throughout human time scales, have sources that might be sequential or mixed, and their potential repercussions can vary significantly. Furthermore, [21] reveals that multi-hazard can be defined as a danger that arises quickly when it occurs suddenly, such as the simultaneous occurrence of earthquakes, volcanic eruptions, or tsunamis. Even though there is no widely agreed-upon concept of a natural hazard, its meaning has been extensively discussed and debated in several fields [5,23].

2.2. Interaction

Various approaches to assessing multi-hazard risk and interactions can be categorized into qualitative, semi-quantitative, and quantitative methods. Qualitative approaches, as described by [7], rely on expert judgment and descriptive methods, while semi-quantitative methods use indices and classifications. Quantitative methods employ numerical data and statistical techniques for precise assessments. [24] identify three main methods for visualizing and constraining hazard interactions: qualitative descriptions and classifications, hazard matrices and diagrams, and probability/scenario trees. [10] further elaborate on quantifying hazard interrelations using matrices, models, and classification methods, including stochastic, empirical, and mechanistic models. These diverse approaches provide a range of tools for understanding and managing the complex interactions between multiple hazards.[10] 's idea of mutual exclusion scenario is also interesting - known as negative dependence - it refers to a situation where two events cannot occur simultaneously and are mutually exclusive (See Table 1).

[24] state that identifying and constraining hazard interactions can help us better understand the hazard potential faced by a region and, thus, the overall risk. Interactions between hazards can occur in various models. Several experts have classified the interrelationships between primary and secondary hazards, as seen in Table 1. Despite growing interest in multi-hazard studies, few studies quantify the dynamic interactions that characterize these phenomena. For example, using the network theory, Dunant et al. 2021 demonstrated the dynamic complexity of natural hazards, it is essential to develop a multi-hazard interaction model with impacts at a desired level for effective emergency planning and resilience assessment.

Table 1. Different interrelation classifications for natural hazards from different sources.

Source	Interaction type
[24]	• *Interactions where a hazard is triggered*: One hazard trigger one (or more) other hazard(s). • *Interactions where the probability of a hazard is increased*: One hazard change environmental parameter that moves toward a change in the likelihood of another hazard. • *Interactions where the probability of a hazard is decreased*: One hazard alters the frequency or magnitude of another.

 doi:10.20944/preprints202406.0868.v1

	• *Events involving the spatial and temporal coincidence of natural hazards*: Two hazards are independent and occur simultaneously by
[5]	• *Independent relationship*: Two hazards are independent. • *Mutex relationship*: Two hazards cannot occur together; their trigger factors are mutually exclusive. • *Parallel relationship*: Two hazards depend on the same trigger factors. • *Series relationship*: One hazards triggers another hazard.
[25]	• *Independent events*: Two hazards are independent. • *Coupled events*: Two hazards are triggered by the same triggering event. • *One hazard changes the conditions for the next*. • *Domino or cascading hazard*: One hazard causes the next.
[10]	• *Independence: Two hazards occur simultaneously without influencing each other.* • *Triggering (Cascading): A primary hazard triggers a secondary hazard and/or tertiary hazard.* • *Compound Hazard: Multiple hazards occur together, arising from a common primary event.* • *Changes in Circumstances: One hazard alters the conditions affecting another hazard.* • *Mutual exclusion: One hazard excludes the possibility of the other hazard happening at the same time.*
[3] De Angeli et al. 2022	• *Parallel hazards*, where the same trigger generates multiple hazards. • *Cascading hazards*, where one adverse event triggers a series of sequential events. • *Disposition alteration*, where the occurrence of one hazard influences the frequency or magnitude of a second hazard. • *Additional hazard potential*, where different hazards occurring in the same space and time amplify each other. • *Coincident triggering*, where two hazards coincide and trigger a third hazard. • *Cyclic triggering*, where the triggering of a second hazard worsens the first hazard, leading to further episodes of the secondary hazard.

2.3. Stages

Multi-hazard risk assessment involves evaluating the specific attributes of each hazardous event, such as likelihood, occurrence rate, and intensity, as well as how these events influence and affect one another [7,26]. The initial stage of hazard risk assessment involves identifying hazards, determining their intensity, and assessing potential damage to evaluate disaster severity [23]. [27] emphasize that effective disaster risk management begins with identifying hazards and determining susceptibility, often through hazard maps that show potential disasters and their interactions.

[10] highlights the importance of examining hazard interactions for accurate multi-hazard risk maps. This approach benefits users by organizing hazard risk information and offering visually informative depictions of potential dangers, which are crucial for disaster risk assessment and planning [28]. Hazard maps also serve as key references for infrastructure construction and urban planning [29].

Eventually, a comprehensive approach that considers the spatial, demographic, and physical contexts and their interconnections and feedback can significantly reduce the human and economic losses caused by a disaster. This approach recognizes that the conditions before a disaster can intensify or lessen its impacts [30]. Although multi-hazard risk analysis offers numerous advantages, its development has various obstacles. [30,31] highlighted that data availability, quality, and accuracy pose significant constraints for multi-hazard research. Furthermore, the scope of analysis is a crucial factor to consider. The stakeholders involved frequently determine the study's scope, and the size of the study area varies depending on the level of detail the researcher needs to present their findings [7]. This may be why the infrequency of conducting multi-hazard risk assessments on small islands may be attributed to this factor.

A comprehensive approach that considers spatial, demographic, and physical contexts, along with their interconnections and feedback, can significantly reduce human and economic losses caused by disasters. This approach acknowledges that pre-disaster conditions can either intensify or mitigate impacts [30]. Interestingly, what is called as ‘pre-disaster’ conditions can often be a result from residual risk from past disasters that can be compounded by future hazard events [32].

 doi:10.20944/preprints202406.0868.v1

Despite the benefits of multi-hazard risk analysis, its development faces several obstacles. [30,31] highlight that data availability, quality, and accuracy are significant constraints for multi-hazard research. Additionally, the scope of analysis is crucial and often determined by the stakeholders involved. The size of the study area varies depending on the level of detail required by the researcher [7]. This may explain why multi-hazard risk assessments are infrequently conducted on small islands.

3. Methods and Geographical Selection

Using both qualitative and quantitative research methods, this study compiles a comprehensive catalogue of multi-hazard disaster risks for Ternate Island. The qualitative information includes history and descriptions of natural hazards. The quantitative approach presents numerical data collected from primary and secondary sources, emphasizing the island's hazards. The research process begins with hazard assessment, identifying and mapping individual hazards, followed by visualizing risk and hazard interactions using a geographical information system (GIS). Additionally, the study examines the exposure of the population and infrastructure to multi-hazard risks.

3.1. Stages in Multi-Hazard Assessment: Focus on Exposure

3.1.1. Generating Individual Hazard Maps

This stage focuses on analysing potential hazards and visualizing individual type hydrometeorological hazards (e.g., flash floods, landslides, extreme waves and abrasion, and extreme weather) and geological hazards (earthquakes, tsunamis, and volcanic eruptions). Initially, individual hazards are mapped according to the guidelines provided by the Indonesian National Disaster Management Agency [33]. Data sources and technical procedures for creating individual hazard maps are obtained from the website https://inarisk.bnpb.go.id/. Table 2 lists the necessary data for creating hazard maps for each type of disaster. The next paragraph will briefly explain the process of creating and analysing the spatial extent of different disaster hazards using ArcGIS 10.8.

Flash floods can be mapped by identifying areas prone to flood inundation using a geomorphological approach to river basins. This approach can be validated with existing data on past flood impact areas. The process begins by segmenting DEM map to determine the extent of the area. Next, the landslide danger map is overlaid onto the river network map to identify primary rivers that have the potential to form natural dams. The elevation of the river and the surrounding buffer zone is then determined to establish the possible extent of flash flood inundation. Finally, the flash flood index is calculated.

Landslide hazard assessments involve identifying regions at risk of slope failure, calculating the likelihood of occurrence, and estimating the potential impact. We will create a landslide hazard map using DEM data and a map indicating areas susceptible to ground movement. First, an analysis of the DEM map will determine slope classes. Slope classes exceeding 45% are then overlaid with the map showing ground movement susceptibility zones. These combined areas are categorized as probable runout zones. Finally, the map is examined to derive a numerical score representing the level of landslide hazard.

Table 2. Data Sources and Type for Individual Hazard Maps.

Data Type	Data Form	Source	FF	LS	EWA	EW	EQ	TS	VO
Administrative Boundaries	Vector	BIG/ BAPPEDA	√	√	√	√	√	√	√
Digital Elevation Model (DEM)	Raster	BIG	√	√	√	√	√	√	
Watershed Boundary Map	Vector	KLHK	√						
River network Map	Vector	BIG	√						
Map of land Movement vulnerability zone	Vector	PVMBG		√					
High wave map	Tabular	BMKG			√				

Preprints.org (www.preprints.org) | NOT PEER-REVIEWED | Posted: 13 June 2024 doi:10.20944/preprints202406.0868.v1

Data Type	Data Form	Source	FF	LS	EWA	EW	EQ	TS	VO
Ocean current speed map	Tabular	BMKG			√				
Geomorphology map	Vector	BIG			√				
Coastline map	Vector	BIG			√			√	
Vegetation cover	Vector	BIG/KLHK			√	√		√	
Annual rainfall map	Vector	BIG/BMKG				√			
Peak ground acceleration map	Vector	PGN					√		
Average-shear wave velocity in the upper 30 m	Tabular	PGN					√		
Maximum tsunami wave	Tabular	BNPB						√	
Volcano disaster risk map	Vector	PVMBG							√

Note: BIG: Geospatial Information Agency; KLHK: Ministry of Environment and Forestry; PVMBG: Volcanology and Geological Hazard Mitigation Centre; BMKG: Meteorological, Climatological, and Geophysical Agency; PGN: National Earthquake Centre; BNPB: National Disaster Management Agency; BAPPEDA: Regional Planning and Development Agency. FF: flashflood; LS: Landslide; EWA: Extreme Wave and Abrasion; EW: Extreme Weather; EQ: Earthquake; TS: Tsunami; VO: Volcano.

Extreme weather, as defined in this study, involves examining hazards associated with severe weather conditions, mainly focusing on powerful winds often accompanied by intense rainfall. Creating hazard maps for extreme weather disasters includes classifying landforms using morphological data, determining land openness through land use maps, classifying slopes with DEM maps, and calculating rain areas based on yearly rainfall maps. After these classifications, the land area undergoes fuzzy overlay and cutting operations to integrate the data. Finally, the danger index is computed, and areas are categorized based on their level of risk.

Extreme coastal wave and abrasion hazards are limited to land areas, focusing on assessing vulnerabilities on land. The measures used assess the extent to which coastal areas are exposed to potential dangers, with initial data including wave height and current speed values. Creating a hazard map involves generating buffers around maps that display wave height, ocean currents, beach typology, vegetation cover, and coastline shape. Land cover significantly impacts exposure likelihood: areas with substantial mangrove forests have a low likelihood, those with bushes have a moderate likelihood, and areas without vegetation have a high likelihood. The Fuzzy approach indexes all characteristics, which are then combined using the Fuzzy Overlay method to determine the index for extreme wave and abrasion hazards. Each parameter is assigned a score and weight based on its impact on the hazard intensity before overlaying.

Earthquakes can escalate into disasters, making earthquake-shaking intensity maps essential for mitigating earthquake risks. Creating these maps involves categorizing topographic features using the DEM map, determining the peak acceleration on bedrock through either earthquake scenario analysis or a probabilistic technique with attenuation distance connections, and calculating surface shaking intensity by multiplying the soil amplification factor by the bedrock shaking intensity. The collected data is then analysed to estimate the peak ground acceleration (PGA), which is used to calculate an earthquake hazard index.

Tsunami hazard distribution is determined through mathematical calculations that account for the decrease in tsunami height per meter of inundation, slope distance, and surface roughness. Creating the danger map begins with categorizing slopes based on the DEM map. Next, a surface roughness coefficient is generated using available land use data, followed by determining the tsunami height loss coefficient and inundation distance. Fuzzy logic is then employed to ascertain the hazard index category.

Volcanic hazard assessment involves assigning a weight to each region based on its susceptibility to volcanic disasters. Volcanic eruption hazard maps are created by integrating data from individual hazard element maps, focusing on the landing and ejection zones. The landing zone includes hazards such as lava flows, pyroclastic flows, toxic gas, eruptive lava, and surges, while the ejection zone involves pyroclastic falls. The analytical results of these two zones are then superimposed to derive a volcanic eruption hazard index.

3.1.2. Generating Multi-Hazard Maps

A multi-hazard map is a map that shows the combination of several risks that occur in the exact location [23]. [34] states that the separate hazard maps are combined into a single integrated hazard map by adding the intensity of the several individual hazards. Consequently, we generated a raster surface for each danger by classifying the severity of the hazard into five ordinal scales ranging from 1 to 3. These scales correspond to the standardized hazard categories of low, moderate, and high, as defined by the National Disaster Management Agency. We utilized the weighted overlay function and Map algebra/raster calculator tool in ESRI's ArcGIS software to superimpose the individual hazard maps. This method considers both the range of values and the number of observations for each category, making it a commonly used approach for classification in mapping [35,36].

Given that the research area is uniformly susceptible to all dangers, we assumed that each hazard carries similar significance. Consequently, we assigned identical weights as specified by the National Disaster Management Agency standardized [33] while creating the integrated hazard map. We generate multi-hazard interaction maps by considering several disasters caused by hydrometeorological events, including floods, landslides, extreme weather hazards, and extreme wave and abrasion events. Meanwhile, an integrated map was created to encompass all types of disasters and their associated risks.

3.1.3. Multi-Hazard Interaction Matrix

In this research, the relationship between hazards is essential. In consideration of the seven hazards (four hydrometeorological hazards and three geological hazards) that occur in the study area, we preferred to implement a hazard diagram and matrix approach, as recommended by [24] and implemented by [37,38]. By analyzing a variety of spatially significant hazards, the hazard matrix method identifies which hazards may precipitate or increase the probability of other hazards. It provides a structured and semi-quantitative method for analyzing and visualizing hazard interactions.

In analysing hazard interactions, we will refer to data from the Regional Disaster Management Agency (BPBD) and previous research on disaster events on Ternate Island. Thus, out of a possible 49 interactions, we identified multiple hazard interactions for each of the seven hazards chosen for this investigation. For guidance on completing the hazard interaction matrix, please consult the work of [24]. The hazards will be designated using a two-letter nomenclature. The vertical axis of the matrix will be utilized to depict the primary hazards, which are the initial hazards that either cause or modify the probability of other hazards transpiring (to be seen Section 4.3 - Figure 6).

3.2. Geographical Context Ternate Island and hazard risk

Ternate Island, covering 9,867 hectares in North Maluku, Indonesia, is characterized by its volcanic nature and unique geomorphology (Figure 1). The island's geological materials are primarily volcanic in origin, formed through recurrent eruptions that deposited pyroclastic flows, lava flows, lahars, and tephra over millennia [39,40]. The island's steep terrain includes slopes exceeding 25%, with inclines over 40% leading to Mount Gamalama's summit, while coastal slopes range from 2% to 8% [40–42]. Ternate also has three lakes—Laguna, Tolire Besar, and Tolire Kecil—formed by the remain active Gamalama volcanic activity located in the eastern and southwestern regions of the island [44].

The National Disaster Management Agency (BNPB) has identified nine potential hazards on Ternate Island, including floods, flash floods, landslides, extreme weather, extreme waves, abrasion, earthquakes, tsunamis, volcanic eruptions, forest fires, and social conflicts [45]. Recent studies have focused on the impacts of specific (single) hazards, including tsunamis [45,46], coastal abrasion [47–

49], volcanic eruptions [51], landslides [42,51], earthquakes [53], floods [53–56], and extreme weather [58].

Administratively, Ternate Island is comprised of 5 sub-districts and 60 villages. All sub-districts and villages are under Ternate city government. In historical records, Ternate Island has been renowned for its economic prosperity since the colonial era. Various European nations, including the Dutch, Spanish, and Portuguese, established trade connections with the Ternate Kingdom specifically for trading spices such as cloves and nutmeg [59]. Therefore, Ternate remains the focal point of economic progress in the province of North Maluku [60]. Ternate is a centre for various economic activities, such as construction, trading, transportation, and various services. These activities are facilitated by constructing various infrastructure on the island, including ports, airports, commercial centres, educational centres, and government centres. Consequently, the economy in the city of Ternate is seeing continuous growth [61]. According to the Central Bureau of Statistics data, the economic growth rate of Ternate in 2023 was 5.0% [17].

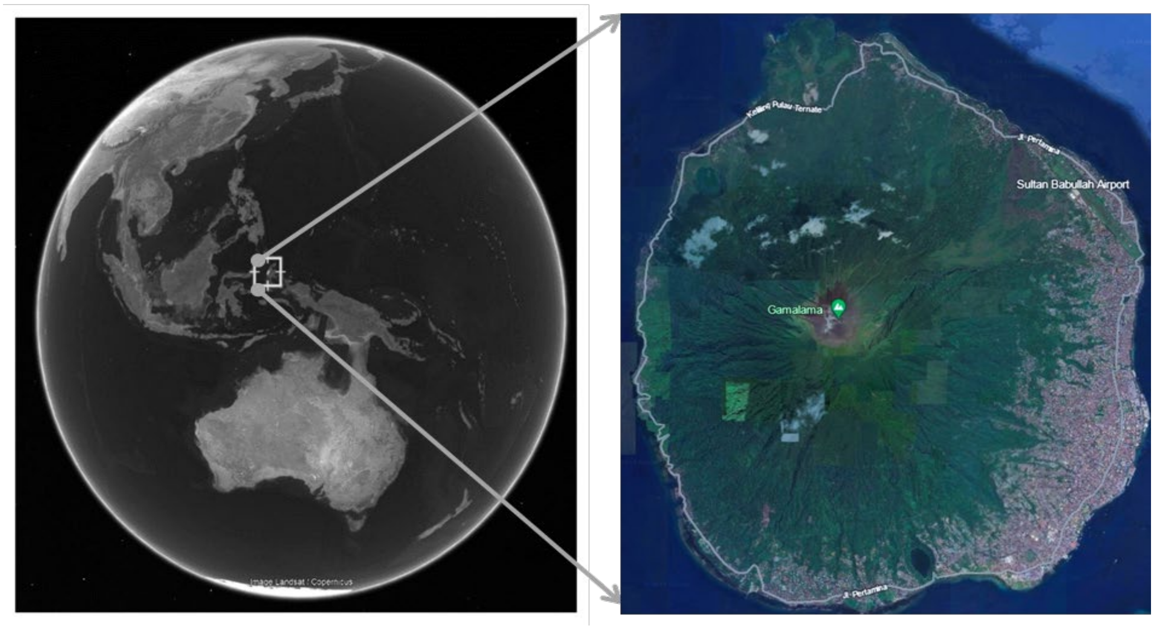

Figure 1. North Maluku and Ternate Island.

3.2.1. Geological Hazard in Ternate Island

Mount Gamalama is situated right at the center of Ternate Island and is well-known for its high level of volcanic activity [43,61]. Historical records indicate that Gamalama volcano has erupted at least 75 times from 1510 to 2015 [43,62]. These eruptions have often been catastrophic. For instance, the volcanic eruption in 1737, 50 years after the 1687 eruption, led to lava flows forming westward, passing settlements, and reaching the sea. Another notable period of volcanic activity spanned 18 years from 1962 to 1980, resulting in a new crater and ash dispersal that blanketed the entirety of Ternate Island with a layer of volcanic ash 10-15 cm thick. Consequently, around 40,000 individuals evacuated to Tidore and the neighboring islands surrounding Ternate [44,63]. In addition, the volcanic eruption in 2011 in Tubo Village resulted in the loss of three lives and the destruction of 78 dwellings [64]. The most recent eruption, observed in 2015, had a rather lengthy period, from July 16 to September 8, 2015, [63].

Since 1858 Ternate has experienced recorded 16 devastating earthquakes with a strength ranging from VI to VIII on the Modified Mercalli strength scale [52,64]. These earthquakes have resulted in the loss of 42 lives and the collapse of numerous houses. According to statistics from the United States Geological Survey (USGS), there were 580 recorded earthquakes with a magnitude of 5 magnitude and a depth of 0-70 km in North Maluku Province from 2000 to 2020 [65,66].

It was estimated that at least 32 tsunami events were recorded in the Maluku Sea between 1600 and 1992, resulting in the deaths of 7,576 individuals. One such catastrophe is the tsunami caused by the Gamalama volcano eruption in 1871, which claimed over 4,000 lives [68]. According to [69], an earthquake and subsequent tsunami on July 14, 1855, killed 24 individuals. The most recent tsunami that impacted North Maluku resulted from a seismic event of Mw 7.2 in 2017, where the earthquake's epicenter was situated in the central region of the Maluku Sea [70].

3.2.2. Hydrometeorological Hazards in Ternate Island

Frequent flash floods due to the topographic characteristics and residual volcanic risk from Gamalama. These floods often occur when cold lava is carried by water down rivers, eventually reaching residential areas [45]. Between December 2011 and May 2012, flash floods resulted in fourteen deaths, displaced 1,040 individuals, and damaged 273 houses to varying degrees [71]. Additionally, four bridges and nine villages across three sub-districts were affected. Historical records also show that flash floods occurred in 1840, 1897, and 1907 [57]. These floods were characterized by loose mud and sand mixed with fragments of andesite and basalt andesite.

Landslides are also common. For example, in 2009, there were six recorded incidents of floods-induced landslides, resulting in 191 damaged houses, six injuries, and 265 displaced people [52]. The landslides affected several villages, including Salahuddin, Rua, Tabam, Takome, and Dorpedu.

Extreme weather events on the island are on the rise. [58] recently reported prolonged heavy rainfall and powerful winds, recording extreme rainfall of 232.0 mm on January 15, 2021, and 170.6 mm on January 16, 2021, at the Gamar Malamo Meteorological Station in North Halmahera. Similarly, at the Sultan Babullah Meteorological Station in Ternate, rainfall on January 15, 2021, was 74.9 mm, and on January 16, 2021, it was 27.0 mm. Additionally, a maximum wind speed of 16 knots was observed at 03.00 WIT on January 16, 2021. This disaster had substantial impacts, leading to tidal waves, floods, landslides, and extensive damage to wave-protecting embankments, settlements, roads, and ports [58].

Extreme waves also frequently hit this region, causing coastal abrasion. [50] discovered a significant increase in abrasion in the western coastal areas of Ternate Island over the past two decades, resulting in a shoreline shift of up to 68.27 meters inland. Additionally, erosion in the waters surrounding the southern area of Ternate Island reduced the coastline by 9.71 to 27.14 meters [48]. The erosion rate on the southwest shore of Ternate Island, recorded from 2011 to 2018, ranged from 0.9 to 19.73 meters per year [46].

3.3. Exposure Analysis: Population and Infrastructures

Exposure analysis is employed to examine the spatial arrangement of individuals, infrastructure, or other valuable assets that are susceptible to danger. Exposure analysis also examines various sectors that could be affected by hazards, including population distribution, the natural environment (like flora, fauna, and conservation areas), the built environment (such as housing and commercial buildings), and essential public infrastructure (including airports, ports, hospitals, and roads) [72].

Three approaches for analysing exposure in a risk area: official statistics analysis, on-site surveys, and remote sensing image analysis [23]. This combination of techniques can be utilized in exposure analysis to provide comprehensive data on hazardous areas.

This study involved the simultaneous consideration of potential exposure to essential facilities and the assessment of land use maps and field observations. This aims to gather data regarding the precise whereabouts and nature of vulnerable critical infrastructure. Meanwhile, "potential population exposure" refers to measuring population density in different regions, which assesses the possible dangers residents face [35]. The population data was acquired from the Ternate City Statistics Bureau in 2023 [17]. Subsequently, we categorized the population exposure classes into three distinct categories (low, moderate, and high) by considering the number of residents or population density in each village. Further, we superimposed the multi-hazard maps onto people density maps and land use maps, with particular emphasis on settlements and critical infrastructure, to guarantee a thorough assessment of high-risk regions in our investigation. The map overlay activity was conducted utilizing the available ArcGIS Map 10.8 tools, as executed by [18].

 doi:10.20944/preprints202406.0868.v1

4. Results

4.1. Hydrometeorological Hazards

Figure 2a–c, and d display maps derived from examining four maps that pertain to hydrometeorology disasters such as flash floods, landslides, extreme weather, and extreme waves and abrasion. Table 3 displays the computed area, measured in hectares (ha), of the hydrometeorological hazard zones for each sub-district and village in the research areas, categorized as low, moderate, and high. Examining the flash flood hazard map (Figure 2a) reveals that regions susceptible to flash floods align with the course of river flow, originating from elevated terrains and extending towards coastal areas. Consequently, regions located in river basins are particularly vulnerable zones. Table 3 reveals that the West Ternate sub-district has a significant potential for flash flood hazards, with a high category hazard area of 327.6 ha. In contrast, the Centre Ternate sub-district has a relatively lower potential for flash flood hazards, with an area of 18.1 ha. Overall, the flash flood hazard area encompasses 12.6% of the entire land area of Ternate Island. The five villages with the most significant flash flood hazard areas are Sulamadaha, with an area of 142.9 ha; Kulaba, with an area of 102.9 ha; Takome, with an area of 99.4 ha; Sasa, with an area of 98.9 ha; and Tabona, with an area of 97.9 ha.

Landslide hazard mapping on Ternate Island involves identifying locations susceptible to landslides using elevation data and maps indicating zones prone to ground movement. The results of spatial map analysis of probable landslide hazards at the research area are depicted in Figure 2b. This map indicates that the slopes leading to the mountain's summit are most susceptible to landslide risk. The region with the highest classification is located in the West Ternate sub-district, covering an area of 1,816.2 ha, followed by the Ternate Islands sub-district, which spans 1,508.3 ha. The high hazard category, measured in hectares, encompasses 52.0% of the total study area. Additionally, the five sub-districts with the largest areas susceptible to landslides are Loto, with an area of 680.9 ha; Rua t, with an area of 483.5 ha; Foramadiahi, with an area of 442.0 ha; Moya, with an area of 410.1 ha; and Fitu, with an area of 369.5 ha. These findings highlight the significant areas at risk for both flash floods and landslides, with particular emphasis on specific sub-districts and villages that are most susceptible to these natural hazards.

This research examines extreme weather risks, focusing on strong winds and rainfall. Jati et al. (2023) describes strong winds as abrupt, circular, spiral-like winds reaching speeds of 40-50 km/hour, dissipating within 3-5 minutes. The Meteorology, Climatology, and Geophysics Agency reports an average monthly rainfall of 181 mm on Ternate Island [17]. Mapping vulnerability to extreme weather, shown in Figure 2c, indicates that all villages possess risk areas, with highly sensitive villages primarily on the east coast. High-risk areas include the North Ternate sub-district (530.7 ha), South Ternate (500.6 ha), and Central Ternate (325.4 ha), covering 16.1% of the island. Villages at high threat include Sango (75.4 ha), Tafure (73.4 ha), Kalamata (60.5 ha), Dufa-Dufa (51.5 ha), and Tarau (50.1 ha).

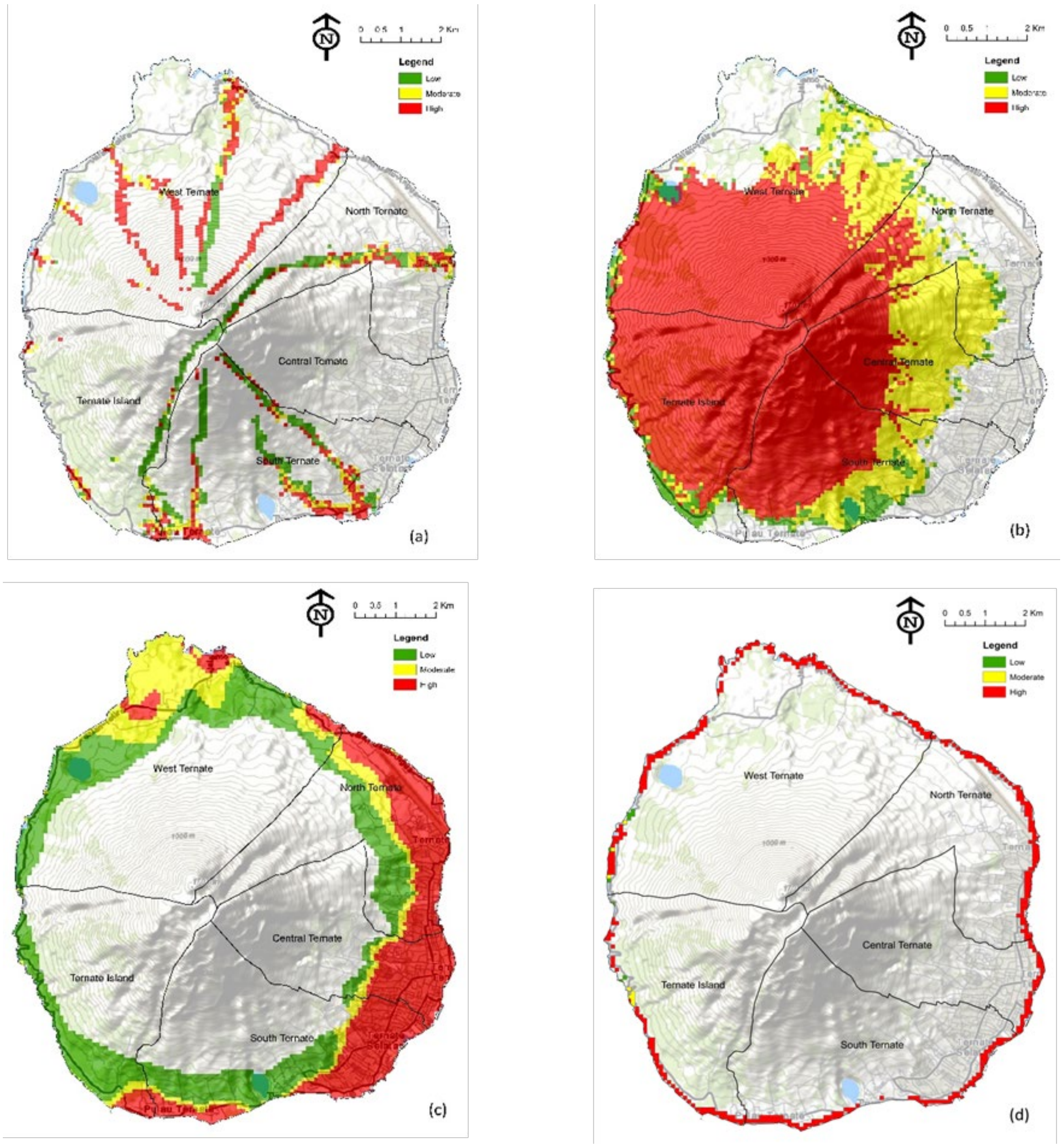

Figure 2. Hydrometeorological Hazard Maps in Ternate Island (**a**) Flash flood; (**b**) Landslide; (**c**) Extreme Weather; and (**d**) Extreme Wave and Abrasion.

[33] also notes that extreme waves, characterized by significant height and generated by wind in shallow waters, can erode coastal areas. Mapping high-risk locations for powerful waves and erosion is conducted in coastal regions. Findings, depicted in Figure 2d, indicate that all sub-districts on Ternate Island, especially coastal areas, are susceptible to severe waves and abrasion. High-hazard areas include the West Ternate sub-district (147.7 ha), North Ternate (95.3 ha), and Central Ternate (35.5 ha), comprising 4.3% of the coastal area. Villages with high extreme wave and abrasion threats are Takome (50.5 ha), Sulamadaha (29.1 ha), Tafure (22.1 ha), Jambula (19.2 ha), and Loto (17.6 ha).

Table 3. The area of hydrometeorological hazards (Ha) for each sub-district and village in low (L), moderate (M), and high (H) categories.

Sub-district/ Village	FF			LS			EW			EWA		
	L	M	H	L	M	H	L	M	H	L	M	H
North Ternate Sub-district												
Akehuda	2.0	5.8	13.0	0.0	0.0	0.0	0.0	0.0	46.4	0.0	0.0	1.7

Preprints.org (www.preprints.org) | NOT PEER-REVIEWED | Posted: 13 June 2024 doi:10.20944/preprints202406.0868.v1

Sub-district/ Village	FF			LS			EW			EWA		
	L	M	H	L	M	H	L	M	H	L	M	H
Dufa-dufa	6.4	9.1	14.2	7.5	16.7	0.0	25.7	9.4	51.5	0.0	0.0	11.5
Kasturian	0.0	0.0	0.0	2.7	19.1	0.0	16.0	6.8	11.2	0.0	0.0	3.3
Salero	0.0	0.0	0.0	0.0	0.0	0.0	0.0	0.0	21.3	0.0	0.0	5.8
Sangaji	0.0	0.0	0.0	4.5	30.5	0.0	22.9	1.9	31.7	0.0	0.0	13.3
Sangaji Utara	0.7	0.0	4.3	10.3	48.9	0.0	44.0	4.0	22.3	0.0	0.0	0.2
Sango	35.1	1.0	8.8	10.9	33.8	124.5	32.9	39.0	75.4	0.0	0.0	14.1
Soa	0.0	0.0	0.0	3.9	24.4	0.0	8.3	7.9	26.6	0.0	0.0	0.0
Soasio	0.0	0.0	0.0	0.0	0.0	0.0	0.0	0.0	18.1	0.0	0.0	5.9
Tabam	0.0	0.0	0.0	0.0	0.0	0.0	0.0	1.0	40.3	0.0	0.0	5.5
Tafure	2.9	2.4	0.3	0.0	0.0	0.0	0.0	0.0	73.7	0.0	0.0	22.1
Tarau	0.6	0.0	0.1	6.2	33.0	104.5	12.4	24.3	50.1	0.0	0.0	9.0
Toboleu	0.0	0.0	0.0	4.4	60.7	0.0	52.2	7.7	20.0	0.0	0.0	2.8
Tubo	39.9	25.7	25.1	11.2	111.4	118.1	58.6	32.9	42.0	0.0	0.0	0.0
Central Ternate Sub-district												
Kalumpang	0.0	0.0	0.0	0.0	0.0	0.0	0.0	0.0	25.2	0.0	0.0	0.0
Kampung Pisang	0.0	0.0	0.0	0.0	0.0	0.0	0.0	0.0	8.3	0.0	0.0	0.0
Kota Baru	0.0	0.0	0.0	0.0	0.0	0.0	0.0	0.0	20.7	0.0	0.0	11.3
Makassar Barat	0.0	0.0	0.0	1.9	5.7	0.0	3.6	7.3	26.2	0.0	0.0	0.0
Makassar Timur	0.0	0.0	0.0	0.0	0.0	0.0	0.0	0.0	17.9	0.0	0.0	4.6
Maliaro	0.0	0.0	0.0	1.0	22.4	11.0	8.6	9.1	49.7	0.0	0.0	0.0
Salahuddin	0.0	0.0	0.0	0.2	0.0	0.0	0.6	4.6	29.9	0.0	0.0	0.0
Santiong	0.0	0.0	0.0	0.0	0.0	0.0	0.0	0.0	25.5	0.0	0.0	0.0
Stadion	0.0	0.0	0.0	0.0	0.0	0.0	0.0	0.0	24.5	0.0	0.0	0.0
Takoma	0.0	0.0	0.0	0.0	0.0	0.0	0.0	0.0	19.7	0.0	0.0	0.0
Tanah Raja	0.0	0.0	0.0	0.0	0.0	0.0	0.0	0.0	8.5	0.0	0.0	0.0
Marikurubu	0.0	0.0	0.0	8.5	136.9	187.4	11.9	8.6	14.3	0.0	0.0	0.0
Muhajirin	0.0	0.0	0.0	0.0	0.0	0.0	0.0	0.0	15.8	0.0	0.0	8.4
Moya	0.0	0.0	0.2	0.3	293.8	116.0	5.8	0.4	0.0	0.0	0.0	0.0
Tongole	3.6	1.0	4.5	1.0	85.6	156.9	11.1	1.5	0.3	0.0	0.0	0.0
Gamalama	0.0	0.0	0.0	0.0	0.0	0.0	0.0	0.0	38.9	0.0	0.0	11.2
South Ternate Sub-district												
Bastiong Karance	0.0	0.0	0.0	0.0	0.0	0.0	0.9	4.1	30.2	0.0	0.0	6.7
Bastiong Talangame	0.0	0.0	0.0	0.0	0.0	0.0	0.0	0.0	37.7	0.0	0.0	4.5
Fitu	0.0	0.0	0.0	29.5	67.2	272.8	97.4	11.1	13.8	0.0	0.0	14.8

Preprints.org (www.preprints.org) | NOT PEER-REVIEWED | Posted: 13 June 2024 doi:10.20944/preprints202406.0868.v1

Sub-district/ Village	FF			LS			EW			EWA		
	L	M	H	L	M	H	L	M	H	L	M	H
Gambesi	36.2	6.6	16.2	15.6	7.4	120.1	44.4	10.3	28.4	0.0	0.0	12.8
Jati	0.0	0.0	0.0	0.0	0.0	0.0	0.9	4.1	30.2	0.0	0.0	0.0
Jati Perumnas	0.0	0.0	0.0	1.6	17.4	0.0	0.8	4.1	34.5	0.0	0.0	0.0
Kalumata	23.2	20.6	34.5	15.1	69.8	69.8	52.3	8.0	60.5	0.0	0.0	11.7
Kayu Merah	4.8	8.2	20.1	1.1	7.4	0.0	7.7	3.6	36.1	0.0	0.0	6.4
Mangga Dua	0.0	0.0	0.0	0.0	0.0	0.0	0.0	0.0	29.6	0.0	0.0	9.0
Mangga Dua Utara	0.0	0.0	0.0	0.0	0.0	0.0	0.0	0.0	32.2	0.0	0.0	5.5
Ngade	26.9	4.8	13.4	59.6	42.4	119.8	65.8	5.0	6.5	0.0	0.0	2.0
Sasa	38.1	24.5	36.3	8.6	4.7	303.7	71.2	11.7	37.5	0.0	0.0	14.4
Tabona	51.8	13.0	33.1	28.5	111.8	103.4	33.0	12.9	18.1	0.0	0.0	0.0
Tanah Tinggi	0.0	0.0	0.0	0.0	0.0	0.0	0.0	0.0	18.4	0.0	0.0	0.0
Tanah Tinggi Barat	0.0	0.0	0.0	0.0	0.0	0.0	3.8	10.1	29.1	0.0	0.0	0.0
Toboko	0.0	0.0	0.0	0.0	0.0	0.0	0.0	0.0	12.1	0.0	0.0	1.9
Ubo-Ubo	8.0	2.4	3.4	0.0	0.0	0.0	0.0	0.0	45.5	0.0	0.0	0.0
West Ternate Sub-district												
Bula	0.0	0.0	0.9	4.4	99.3	128.2	43.6	18.5	7.6	0.0	0.0	6.7
Kulaba	0.0	4.0	98.9	16.5	164.6	136.8	39.8	19.5	24.7	0.0	0.0	10.9
Loto	1.0	12.0	61.8	9.7	8.0	663.2	110.9	1.9	0.0	4.0	1.0	17.6
Sulamadaha	38.6	25.0	79.3	18.4	101.3	181.3	131.6	145.4	41.1	0.0	0.0	29.1
Takome	0.0	16.0	83.4	35.6	20.1	257.7	220.6	300.7	46.6	0.0	0.0	50.5
Tobololo	30.4	0.0	0.4	36.2	79.9	139.1	91.5	0.9	0.0	0.0	0.0	11.8
Togafo	0.0	1.0	3.0	16.1	9.1	310.0	62.7	0.1	0.0	1.6	2.0	12.6
Ternate Island Sub-district												
Afe-Taduma	0.0	3.0	4.9	3.9	4.6	336.9	30.2	1.3	0.0	0.6	0.0	7.9
Dorpedu	0.0	0.0	0.0	1.6	0.5	196.8	30.1	0.9	0.0	1.6	0.0	4.0
Foramadiahi	72.8	4.1	4.0	0.0	0.0	442.0	11.7	0.0	0.0	0.0	0.0	0.0
Jambula	2.8	8.8	16.0	12.8	6.1	18.4	43.2	19.8	49.3	0.0	0.0	19.2
Kastela	2.0	5.4	9.9	61.4	18.1	54.7	131.5	3.8	0.0	0.0	0.0	16.2
Rua	0.0	0.6	2.9	15.4	8.5	459.5	71.2	0.0	0.0	0.0	5.5	16.9
Total Area	**427.9**	**204.9**	**592.8**	**465.9**	**1771.0**	**5132.7**	**1711.8**	**764.3**	**1526.0**	**7.7**	**8.5**	**423.6**

4.2. Geological Hazards

Figure 3a–c depict the geohazard mapping analysis for earthquakes, tsunamis, and volcanic eruptions at the research location. Table 4 displays the computed area, measured in hectares (ha), of the hydrometeorological hazard zones for each sub-district and village in the research areas, categorized as low, moderate, and high. [30] emphasizes the importance of earthquake shaking

 doi:10.20944/preprints202406.0868.v1

intensity maps in reducing seismic risks. The earthquake hazard mapping in Figure 3a shows that all village areas on Ternate Island are potentially affected by earthquakes: 25.4% low, 29.2% moderate, and 45.6% high. The five villages with the highest earthquake danger are Takome (791.6 ha), Loto (615.2 ha), Sulamadaha (586.8 ha), Rua (482.1 ha), and Foramadiahi (441.9 ha).

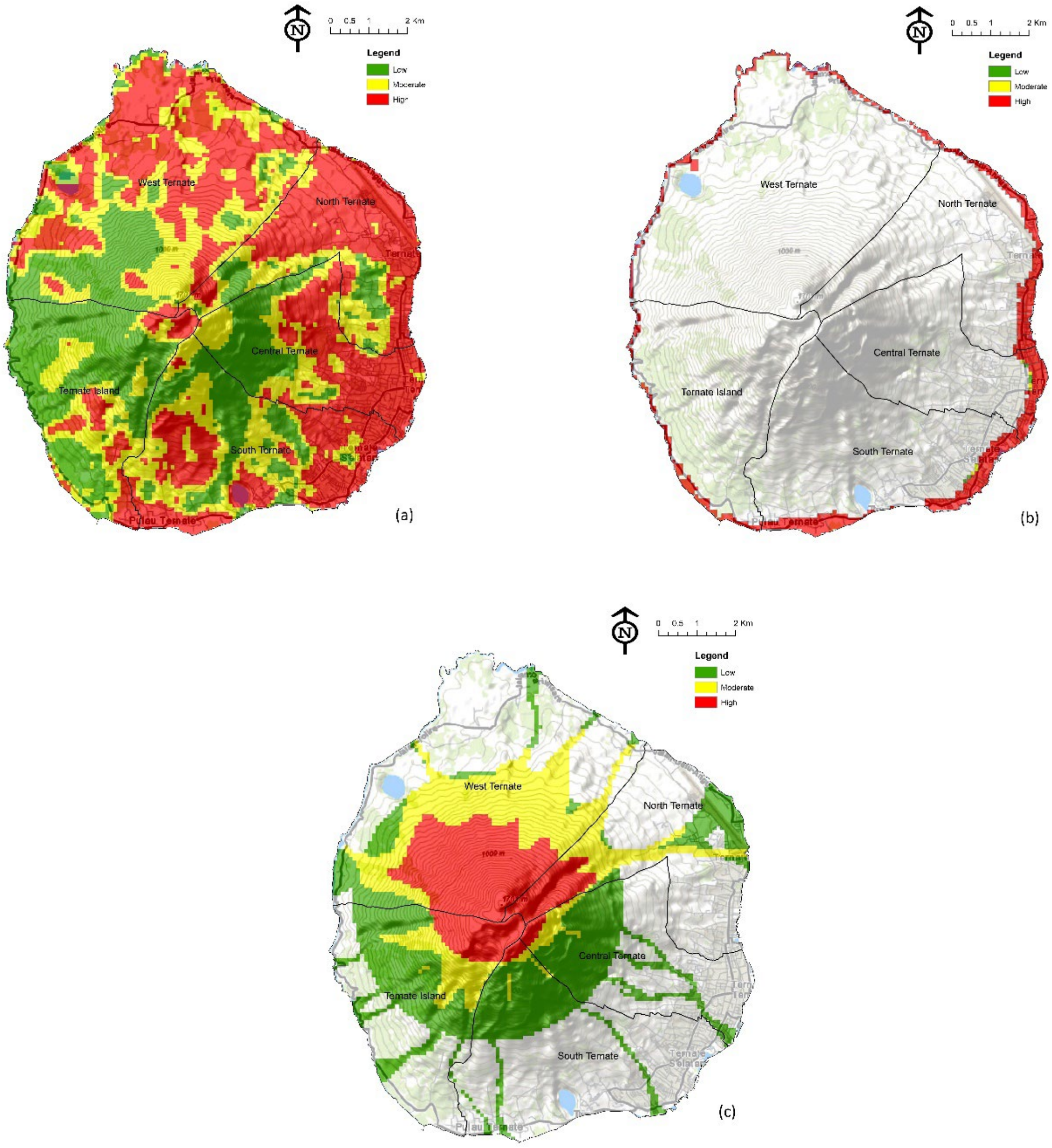

Figure 3. Geological Hazard Maps in Ternate Island a) Earthquake; b) Tsunami; c) Volcano.

The tsunami hazard map in Figure 3b indicates that all coastal areas on Ternate Island are at risk of tsunamis, while mountainous villages are comparatively safer. The hazard area distribution is 0.05% low, 0.08% moderate, and 6.9% high. The villages most prone to tsunamis are Takome (45.3 ha), Gambesi (35.5 ha), Gamalama (34.3 ha), Tafure (31.6 ha), and Kastela (29.4 ha).

Volcanic hazard mapping in Figure 3c shows that zones within 1-2 km from the volcano's crater and along river flows are most at risk. High and moderate risk areas are mainly in West Ternate, North Ternate, and Ternate Island sub-districts, with low risk in South and Central Ternate. The low-hazard category covers 21.8% of the area, moderate 14.5%, and high 12.2%. The most vulnerable villages are Loto (566.3 ha), Foramadiahi (325.6 ha), Togafo (319.1 ha), Rua (303.12 ha), and Afe Taduma (272.7 ha).

By analyzing the outcomes of individual hazard mapping, specific village areas at risk of various disasters can be identified. Hydrometeorological disasters, particularly flash floods, are possible in 32 villages within the study location. Landslides have the potential to occur in 37 villages, extreme

Preprints.org (www.preprints.org) | NOT PEER-REVIEWED | Posted: 13 June 2024 doi:10.20944/preprints202406.0868.v1

weather disasters can happen in all villages, and extreme wave and abrasion disasters are possible in 42 coastal villages on Ternate Island. For geological disasters, earthquakes could affect all villages within the research locations, tsunamis are projected to impact 46 villages, and volcanic disasters have the potential to affect 39 villages. Figure 4 illustrates the number of villages and their susceptibility to these disasters.

Table 4. The area of geological hazards (Ha) for each sub-district and village in low (L), moderate (M), and high (H) categories.

Sub-district/	EQ			TS			VO		
Village	L	M	H	L	M	H	L	M	H
North Ternate Sub-district									
Akehuda	0.0	0.0	46.2	0.0	0.0	35.6	124.6	73.4	127.6
Dufa-dufa	21.9	10.3	54.5	0.0	0.0	29.3	183.9	32.8	56.0
Kasturian	1.7	28.8	13.2	0.0	0.0	20.6	0.0	0.0	0.0
Salero	0.0	3.8	17.7	0.0	0.0	13.1	0.0	0.0	0.0
Sangaji	17.3	9.9	40.0	0.0	0.0	12.7	0.0	0.0	0.0
Sangaji Utara	17.3	32.7	36.5	0.0	0.0	12.2	51.9	4.5	7.5
Sango	22.6	29.8	280.4	0.0	0.0	10.5	32.9	0.0	0.0
Soa	9.1	40.4	14.4	0.0	0.0	10.2	0.0	0.0	0.0
Soasio	0.0	0.0	17.5	0.0	0.0	9.3	0.0	0.0	0.0
Tabam	0.0	0.0	41.3	0.0	0.0	6.7	22.9	0.0	0.0
Tafure	0.0	0.8	73.8	0.0	0.0	4.3	14.0	0.0	0.0
Tarau	12.5	56.7	161.4	0.0	0.0	2.7	9.3	0.0	0.0
Toboleu	35.8	38.3	17.7	0.0	0.0	2.0	0.0	0.0	0.0
Tubo	25.6	99.6	214.4	0.0	0.0	0.0	0.6	0.0	0.0
Central Ternate Sub-district									
Kalumpang	0.0	0.0	25.2	0.0	0.0	0.0	13.7	132.9	74.8
Kampung Pisang	0.0	0.0	8.3	0.0	0.0	0.0	150.9	24.8	7.2
Kota Baru	0.0	0.0	21.3	0.0	0.0	18.6	3.6	132.7	31.6
Makassar Barat	2.9	6.5	31.9	0.0	0.0	16.8	0.0	0.0	0.0
Makassar Timur	0.0	0.0	17.9	0.0	0.0	16.4	0.0	0.0	0.0
Maliaro	0.8	15.4	81.5	0.0	0.0	0.0	107.5	1.5	5.6
Salahuddin	0.0	0.2	34.8	0.0	0.0	0.0	73.1	0.7	0.0
Santiong	0.0	0.0	25.5	0.0	0.0	0.0	0.0	0.0	0.0
Stadion	0.0	0.0	24.5	0.0	0.0	9.2	0.0	0.0	0.0
Takoma	0.0	0.0	19.7	0.0	0.0	4.2	12.7	0.0	0.0
Tanah Raja	0.0	0.0	8.5	0.0	0.0	3.7	0.0	0.0	0.0
Marikurubu	150.8	104.3	107.2	0.0	0.0	0.0	6.2	27.2	73.3
Muhajirin	0.0	0.0	15.7	0.0	0.0	15.8	0.0	0.0	0.0
Moya	114.2	97.1	204.5	0.0	0.0	0.0	1.3	43.8	47.8
Tongole	114.2	115.3	17.3	0.0	0.0	0.0	0.0	1.3	0.0
Gamalama	0.0	6.0	32.2	0.0	0.0	23.5	0.0	0.0	0.0
South Ternate Sub-district									
Bastiong Karance	0.0	5.2	30.2	0.1	0.5	14.3	0.0	0.0	0.0
Bastiong Talangame	6.9	7.1	23.3	3.0	2.3	29.0	0.0	0.0	0.0
Fitu	100.0	161.0	144.8	0.0	0.0	25.6	69.1	123.3	65.0
Gambesi	25.8	55.8	101.0	0.0	0.0	21.8	42.8	128.1	72.2
Jati	0.2	9.0	20.4	0.0	0.0	0.0	0.0	0.0	0.0

Preprints.org (www.preprints.org) | NOT PEER-REVIEWED | Posted: 13 June 2024 doi:10.20944/preprints202406.0868.v1

Sub-district/	EQ			TS			VO		
Village	L	M	H	L	M	H	L	M	H
Jati Perumnas	0.2	9.5	25.1	0.0	0.0	0.0	0.0	0.0	0.0
Kalumata	81.4	98.7	39.5	1.2	0.0	19.7	198.7	24.5	4.8
Kayu Merah	2.3	3.9	41.4	0.8	3.0	15.2	137.2	16.1	18.5
Mangga Dua	0.1	4.2	25.7	0.0	0.5	15.3	0.0	0.0	0.0
Mangga Dua Utara	0.0	0.9	30.5	0.0	0.0	15.8	0.0	0.0	0.0
Ngade	82.2	60.6	76.1	0.0	0.0	15.0	76.6	10.0	4.0
Sasa	64.2	146.6	152.5	0.0	0.0	10.4	13.0	15.1	0.0
Tabona	75.8	90.3	65.0	0.0	0.0	0.0	11.5	3.0	0.0
Tanah Tinggi	0.0	0.0	18.4	0.0	0.2	3.3	10.1	0.0	0.0
Tanah Tinggi Barat	0.0	3.0	40.0	0.0	0.0	0.0	0.0	0.0	0.0
Toboko	0.0	0.0	11.8	0.0	0.0	2.4	3.7	0.0	0.0
Ubo-Ubo	0.0	0.2	44.7	0.0	0.0	0.1	0.1	0.0	0.0
West Ternate Sub-district									
Bula	17.3	89.1	185.4	0.0	0.0	31.6	119.3	92.1	107.7
Kulaba	46.1	191.9	136.6	0.0	0.0	17.9	150.5	0.7	0.0
Loto	286.2	210.7	188.3	0.0	0.5	17.4	85.7	37.3	18.9
Sulamadaha	10.8	207.8	368.2	0.0	0.0	8.3	25.7	0.0	0.0
Takome	115.9	205.2	470.5	0.0	0.5	3.5	11.5	0.0	0.0
Tobololo	4.0	109.7	189.9	0.0	0.0	2.0	3.0	0.0	0.0
Togafo	228.4	78.8	27.2	0.0	0.0	1.0	3.0	0.0	0.0
Ternate Island Sub-district									
Afe-Taduma	327.0	18.6	1.1	0.0	0.0	45.4	72.1	152.2	342.0
Dorpedu	129.3	70.2	0.8	0.0	0.0	29.4	219.7	71.6	11.9
Foramadiahi	172.6	167.8	101.5	0.0	0.0	0.0	18.6	164.1	69.9
Jambula	24.8	27.4	60.1	0.0	0.0	20.9	0.0	0.0	0.0
Kastela	96.2	31.3	8.2	0.0	0.0	20.8	5.5	109.9	57.4
Rua	266.0	113.6	69.3	0.0	0.0	13.7	64.6	9.0	4.0
Total Area	**2710.1**	**2873.9**	**4402.3**	**5.1**	**7.5**	**677.1**	**2151.2**	**1432.5**	**1207.8**

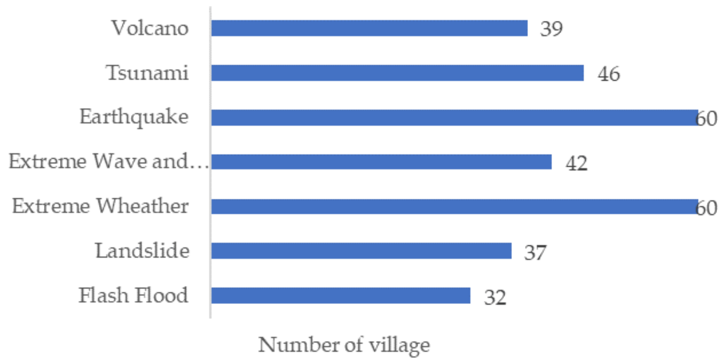

Figure 4. Number of villages with potential hazards.

4.3. Multi-Hazard Maps Assessment

We conducted an analysis and created a map of MCC showing interactions and categorizing them into two groups: interactions between hydrometeorological disasters (such as flash floods, landslides, extreme weather, and extreme waves and abrasion) and interactions involving all types of disasters. Figure 5a,b display the outcomes of the hazard interaction mapping.

Preprints.org (www.preprints.org) | NOT PEER-REVIEWED | Posted: 13 June 2024 doi:10.20944/preprints202406.0868.v1

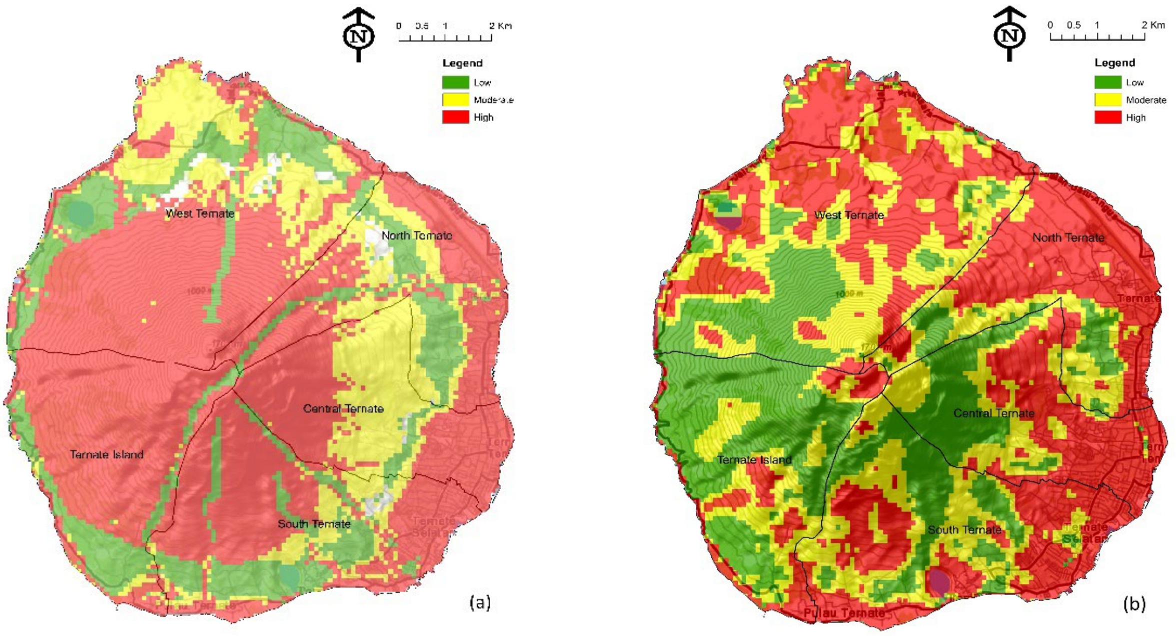

Figure 5. Multi-hazard maps of Ternate Island, a) Hydrometeorological hazards, b) all potential hazards.

According to the meteorological multi-hazard map depicted in Figure 5a, all villages on Ternate Island are susceptible to hydrometeorological hazards. The danger area calculations indicate that the low danger category covers 21% of the island, the moderate danger category covers 18%, and the high danger category covers 61%. The five villages with the largest hazardous zones are Takome (751.6 ha), Loto (711.6 ha), Sulamadaha (640.7 ha), Fitu (446.7 ha), and Foramadiahi (431.1 ha).

Similarly, the multi-hazard map for all types of hazards depicted in Figure 5b shows that all villages on Ternate Island are susceptible to all disasters. The calculations reveal that the low hazard category encompasses 20% of the island, the moderate danger category covers 29%, and the high danger category accounts for 51%.

The idea of MCC can briefly represented in Figure 6 as it suggests the outcomes of the hazard interaction matrix analysis, identifying 18 interactions within the 7 x 7 matrix. These interactions suggest that hydrometeorological and geological hazards, or a combination of both, can cause a domino effect, where one hazard triggers another sequentially.

According to Figure 6, 16 interactions (32.6%) show a primary hazard increasing the likelihood of a secondary hazard, 2 interactions (4%) show a primary hazard triggering a secondary hazard without increasing its likelihood, and no interactions show an increased likelihood without triggering. Light-grey shading indicates that a primary hazard might trigger a small number of secondary hazards, such as a landslide causing a single flash flood. Dark grey shading indicates that a primary hazard could trigger multiple secondary hazards, like extreme weather causing flash floods, landslides, extreme waves, and abrasion. The thin vertical strip shows that certain hazards have occurred on Ternate Island but have not been recorded by BPBD or previous studies.

The mapping of human exposure and infrastructure offers a detailed view of where population densities and land use intersect with hazard risks, allowing for local hazard exposure analysis for each village and sub-district. Table 5 shows that Ternate Island's 2023 population is 191,712, with 96,131 men, 95,581 women, and 57,757 households. Figure 6 maps population exposure and key infrastructure locations, revealing that the population is mainly concentrated along the eastern coastline in North, Central, and South Ternate sub-districts. Ten villages with significant population exposure are Kalumata, Maliaro, Jati, Sangaji, Marikurubu, Makkasar Barat, Toboleu, Salahuddin, and Makassar Timur.

Preprints.org (www.preprints.org) | NOT PEER-REVIEWED | Posted: 13 June 2024 doi:10.20944/preprints202406.0868.v1

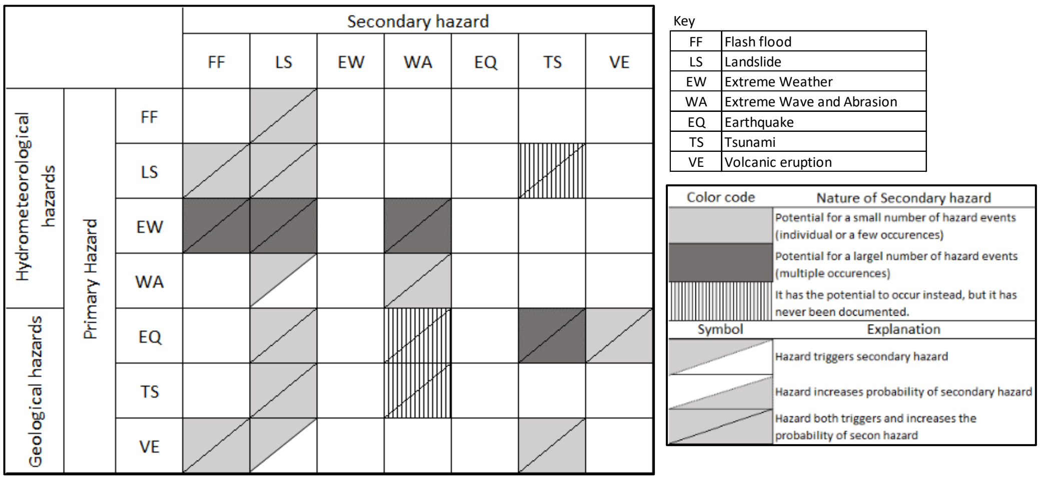

Figure 6. Identification of hazard interactions. A 7 × 7 matrix with primary hazards on the vertical axis and secondary hazards on the horizontal axis.

The overlay results for vital infrastructure, as seen in Figure 7, indicate that significant at-risk facilities include airports, power plants, fuel depots, economic zones, office complexes, tourist destinations, seaports, road networks, and residential neighborhoods. If a disaster strikes, the presence of this infrastructure will result in significant economic losses.

Table 4. Number of Population (male, female, and household) and exposure level in Ternate Island.

Sub-district/ Village	Male	Female	Population	Household	Sex ratio	Exposure level
North Ternate Sub-district						
Akehuda	1825	1739	3564	1110	104.9	High
Dufa-dufa	2651	2744	5395	1652	96.6	High
Kasturian	1767	1733	3500	1044	102.0	High
Salero	1541	1553	3094	969	99.2	High
Sangaji	2991	2841	5832	1796	105.3	High
Sangaji Utara	1977	1968	3945	1197	100.5	High
Sango	898	910	1808	568	98.7	Moderate
Soa	2236	2272	4508	1371	98.4	High
Soasio	978	913	1891	598	107.1	Moderate
Tabam	848	829	1677	497	102.3	Moderate
Tafure	1843	1733	3576	1123	106.3	High
Tarau	733	669	1402	391	109.6	Moderate
Toboleu	2768	2674	5442	1588	103.5	High
Tubo	1479	1515	2994	840	97.6	Moderate
Central Ternate Sub-district						
Kalumpang	1945	1927	3872	1223	100.9	High
Kampung Pisang	1081	1084	2165	690	99.7	Moderate
Kota Baru	1507	1496	3003	947	100.7	High
Makassar Barat	2584	2894	5478	1544	89.3	High
Makassar Timur	2699	2630	5329	1717	102.6	High
Maliaro	3600	3618	7218	2175	99.5	High
Salahuddin	2587	2558	5145	1580	101.1	High
Santiong	1999	1969	3968	1323	101.5	High
Stadion	707	744	1451	467	95.0	Moderate
Takoma	944	955	1899	591	98.8	Moderate

Sub-district/ Village	Male	Female	Population	Household	Sex ratio	Exposure level
Tanah Raja	478	550	1028	346	86.9	Moderate
Marikurubu	2816	2771	5587	1617	101.6	High
Muhajirin	846	766	1612	523	110.4	Moderate
Moya	1285	1208	2493	699	106.4	Moderate
Tongole	604	706	1310	302	85.6	Moderate
Gamalama	1317	1303	2620	859	101.1	Moderate
South Ternate Sub-district						
Bastiong Karance	2329	2383	4712	1456	97.7	High
Bastiong Talangame	2542	2490	5032	1566	102.1	High
Fitu	1974	1966	3940	1159	100.4	High
Gambesi	1275	1198	2473	721	106.4	Moderate
Jati	3433	3458	6891	1945	99.3	High
Jati Perumnas	1436	1448	2884	900	99.2	Moderate
Kalumata	5511	5482	10993	3220	100.5	High
Kayu Merah	2513	2493	5006	1527	100.8	High
Mangga Dua	1628	1614	3242	1040	100.9	High
Mangga Dua Utara	1892	1929	3821	1221	98.1	High
Ngade	1474	1434	2908	808	102.8	Moderate
Sasa	1455	1519	2974	884	95.8	Moderate
Tabona	2495	2400	4895	1358	104.0	High
Tanah High	1724	1750	3474	1066	98.5	High
Tanah High Barat	1575	1521	3096	911	103.6	High
Toboko	1027	1034	2061	654	99.3	Moderate
Ubo-Ubo	1330	1347	2677	829	98.7	Moderate
West Ternate Sub-district						
Bula	498	465	963	304	107.1	Low
Kulaba	960	932	1892	475	103.0	Moderate
Loto	486	503	989	306	96.6	Moderate
Sulamadaha	991	935	1926	567	106.0	Moderate
Takome	555	591	1146	342	93.9	Moderate
Tobololo	689	722	1411	356	95.4	Moderate
Togafo	381	392	773	217	97.2	Low
Ternate Island Sub-district						
Afe-Taduma	500	491	991	304	101.8	Low
Dorpedu	341	316	657	218	107.9	Low
Foramadiahi	592	580	1172	337	102.1	Moderate
Jambula	1616	1471	3087	893	109.9	High
Kastela	597	616	1213	343	96.9	Moderate
Rua	778	829	1607	483	93.8	Moderate

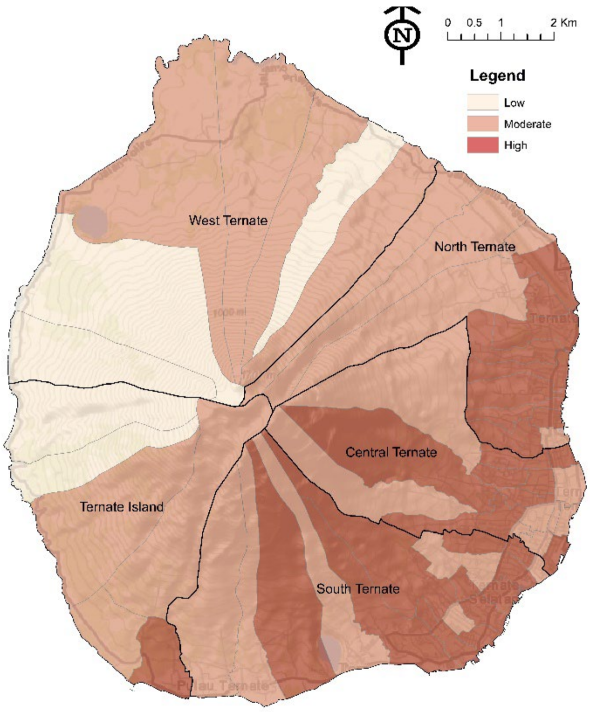

Figure 6. Population Exposure Maps on Ternate Island.

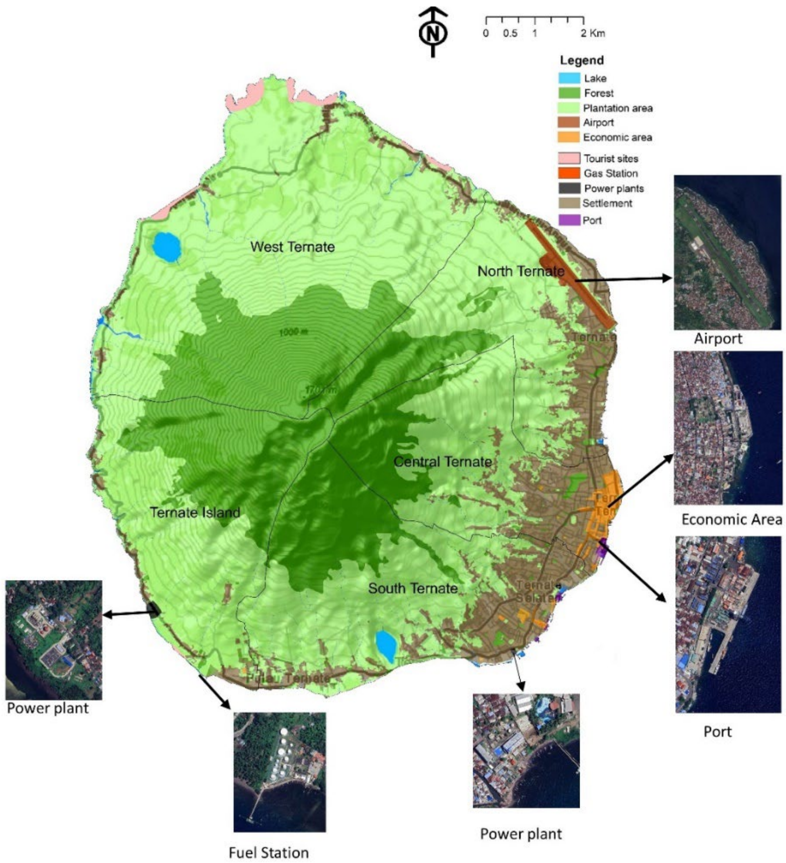

Figure 7. Infrastructures Exposure Maps on Ternate Island.

5. Discussion

The individual hazard map identifies areas within the study location, at both village and sub-district levels, that fall into high, moderate, and low risk categories. Coastal villages face higher risks

 doi:10.20944/preprints202406.0868.v1

of tsunamis, strong waves, and abrasion, while hilly areas are more prone to landslides, flash floods, and volcanic activity. Any area can experience earthquakes and severe weather. This information is crucial for developing tailored disaster mitigation and policy responses by local and national governments.

The results suggest that Ternate Island is highly prone to compounding risk from hydrometeorological and geological hazards. Ternate Island physical characteristics including the geological conditions will continue to shape risk posed on the population and infrastructure built on the island. The island's proximity to the Pacific Ocean also contributes to the incidence of hydrometeorological hazards. [42] noted that climate change affects rainfall distribution on Ternate Island. The warming sea surface temperatures and the reccurent El Nino-Southern Oscillation (ENSO) phenomenon in the Pacific Ocean can lead to more rainfall in the Maluku region [72,73]. Although Ternate is not directly in the path of tropical cyclones, its proximity to cyclone origin areas in the East Pacific occasionally results in cyclone winds affecting the region [33].

The combination of geomorphological conditions, land use changes, and rainfall on Ternate Island increases its susceptibility to landslides [42,51]. Landslides are more likely on sloping landforms such as hills or mountains or in areas where the land shape can be altered to form steep slopes. The landslide hazard level on Ternate Island is characterized by slopes ranging from 15% to 45%. Furthermore, [75] states that mountainous or hilly regions are complex and vulnerable ecosystems frequently impacted by climate change. These areas face primary risks from hydro-meteorological events such as floods, landslides, and debris flows, often accompanied by geological hazards like earthquakes. Due to these conditions, Ternate Island periodically experiences flash floods, landslides, severe weather, strong waves, and erosion.

This study also indicates that Ternate Island is susceptible to multi-hazard interaction in the future. The multi-hazards matrix (Figure 6) shows how different hazards might interact. Table 5 depicts the occurrence of hazards and their interaction on Ternate Island based on the available data. These interactions can be broken down into triggering/cascading and compound hazards.

The hazard interaction matrix highlights potential dangers (thin vertical strip) on Ternate Island, based on existing literature and studies. For example, [76] reported a submarine landslide in eastern Indonesia that triggered a tsunami. Additionally, [69] noted tsunamis triggering extreme waves and abrasion. Table 5 suggests that the occurrence of one disaster often triggers or affects the next, resulting in interactions between them. Landslides, severe weather, and volcanic eruptions are major causes of flash floods, such as those on Ternate Island in 2011 and 2012 [56,70]. Extreme waves and abrasion are linked to severe weather conditions [58]. Tsunamis are associated with earthquakes and volcanic eruptions impacting Ternate Island [69].

Regarding the population exposure map, villages with high population density are high-risk, while those with low density are low-risk. [77] note that rising population density increases exposure, worsened by urbanization and relocation to high-risk areas. Evaluating existing infrastructure vulnerability is crucial for planning and predicting potential losses. Thus, hazard maps are essential for infrastructures evaluation. Due to its small size and distinct geomorphology, Ternate faces challenges in constructing infrastructure and dwellings, exacerbated by population growth and societal progress. Studies by [59,77] indicate that increased demand for land has led to significant alterations in coastal areas. [79] project that by 2030, Ternate will need 96,089 housing units, occupying 960.89 ha. Between 2013 and 2023, residential development in coastal areas rose by 15.69% to 19.69%, especially in South, Central, and North Ternate [80].

Table 5. The hazards and their interaction on Ternate Island.

Primary hazard	Secondary hazard	Type of Interaction	Occurrence	Source
Flash Flood	Landslide	Triggering/ Cascading	February 28, 2020, at Bula village; July 27, 2020, at Tobololo village; January 25, 2021, at Fitu village; April 12, 2021, at Salahuddin village	[81]

Landslide	Flash flood	Triggering/ Cascading	occurred in 2011 and 2012 at Tubo villages;	[57,71,81]
Extreme weather (heavy rain)	Flood - Landside	Compound hazard	June 19, 2020, at Takome village; September 16, 2020, at Rua village; October 15, 2020, at Tabam village; November 14, 2020, at Bastiong Talangame village; November 30, 2020, at Makassar Barat village; January 19, 2021, at Jati village; June 15, 2021, at Soa village.	[81]
Extreme weather (strong wind)	High wave	Triggering/ Cascading	occurred in 2021	[82]
Extreme weather (strong wind)	High wave - Abrasion	Compound hazard	occurred on coastal area in Ternate Island; August 5, 2020, at Sulamadaha village; February 1, 2021, at Tafure village	[47,48,80,82]
Extreme Wave and Abrasion	Landslide	Triggering/ Cascading	August 24, 2020, at Sulamadaha village; March 8, 2021, at Togafo village	[81]
Earthquake	Tsunami	Triggering/ Cascading	North Maluku area; Ternate Island	[67,68]
Earthquake	Tsunami-Landslide	Triggering/ Cascading	Ternate island	[69]
Earthquake	Volcano eruption	Triggering/ Cascading	Ternate island	[50,61]
Volcano eruption	Flash Flood	Triggering/ Cascading	occurred in 2011 and 2012 at Tubo villages;	[56,70,80,83]
Volcano eruption	Tsunami	Triggering/ Cascading	Ternate island	[69]

This has led to significant land use changes on Ternate Island, including coastal land reclamation for business centers [84,85] and deforestation near Mount Gamalama's summit. The forest area decreased from 6,937.3 ha in 2010 to 5,592.8 ha within a decade [78]. Small islands like Ternate face environmental issues such as land degradation and biodiversity loss due to their limited size, isolation, and susceptibility to natural disasters, worsened by population growth and urbanization, infrastructure development and urban planning [29].

6. Conclusions and Limitations

This article showcases the practicality of using a multi-hazard map at the local level to detect the population's exposure and existing infrastructure. The purpose is to utilize this information for sustainability planning, practical demonstration of land-use exposure assessment, and the proposal of a database for risk assessment. Therefore, it is crucial for spatial planning to consider the risks posed by many hazards when making decisions to reduce potential losses that may occur in future extreme events.

The multi-hazard mapping results indicate that the impact of this hazard is becoming more extensive and encompasses the entire territory of Ternate Island, including both hydrometeorological dangers and all other hazards. This is demonstrated by the substantial proportion of land classified as high-risk category, which accounts for up to 61% of the entire area of Ternate Island. Having a disaster risk reduction plan in place anticipating cascading and compounding risk from multi-hazard hazards is pivotal for small island communities. Multi-hazard zonation in SICs is a fundamental step to manage disaster risk. It allows the government and all stakeholders to select and prioritize the dangers that need the greatest attention, allocate different sources, and create an increased resilience system for multi-hazards disruptive scenarios.

While these multi-hazard analysis interaction and mapping provide information about the location and severity of individual hazards, they do not include any data on risk assessment, making them solely danger maps rather than risk maps. Therefore, additional research on risk analysis in these areas is crucial. The author acknowledges the presence of limitations in this research. The approach is incomplete in providing a thorough understanding of disaster risk since it only focuses on creating a list of hazards and disasters without considering other factors. The article does not cover the analysis of vulnerability, capacity, community preparedness, and estimates of all risk components. Another possible drawback is that the availability and accessibility of data might be troublesome in certain cases. This research exclusively utilized data the researcher could obtain from various sources, as the local government lacks a centralized disaster database. We recommend implementing a resilience-enhancing strategy to address multi-hazard situations by examining the consequences of many systems, including their physical, technological, environmental, and social aspects. It is extremely beneficial for further, more detailed, or thorough catastrophe risk assessments.

Author Contributions: Conceptualization, M.R.L and J.L methodology, M.R.L and J.L.; software, M.R.L.; validation, J.L. and K.K.Z.; formal analysis, M.R.L.; investigation, M.R.L.; resources, J.L. and K.K.Z.; data curation, M.R.L.; writing—original draft preparation, M.R.L.; writing—review and editing, J.L. and K.K.Z; visualization, M.R.L.; supervision, J.L. and K.K.Z..; project administration, M.R.L. All authors have read.

Funding: This research received no external funding

Institutional Review Board Statement: The study was conducted in accordance with the Declaration of Human Research Ethics Committee, Research Integrity and Ethics, Research and Innovation, Charles Darwin University (Protocol code H23043/29 June 2023).

Data Availability Statement: The authors will make the raw data supporting this article's conclusions available upon reasonable request.

Conflicts of Interest: The authors declare no conflicts of interest.

References

1. S. Lamichhane *et al.*, "Assessing the prospects of transboundary multihazard dynamics: The case of bhotekoshi—Sunkoshi watershed in sino—Nepal border region," *Sustainability (Switzerland)*, vol. 13, no. 7, Apr. 2021. https://doi.org/10.3390/su13073670.
2. UNDRR, "National Disaster Risk Assessment Words into Action Guidelines Governance System, Methodologies, and Use of Results," 2017. Accessed: May 25, 2023. [Online]. Available: https://www.unisdr.org/files/52828_nationaldisasterriskassessmentpart1.pdf.
3. S. De Angeli, B. D. Malamud, L. Rossi, F. E. Taylor, E. Trasforini, and R. Rudari, "A multi-hazard framework for spatial-temporal impact analysis," *International Journal of Disaster Risk Reduction*, vol. 73, Apr. 2022. https://doi.org/10.1016/j.ijdrr.2022.102829.
4. M. Bordbar, H. Aghamohammadi, H. R. Pourghasemi, and Z. Azizi, "Multi-hazard spatial modeling via ensembles of machine learning and meta-heuristic techniques," *Sci Rep*, vol. 12, no. 1, Dec. 2022. https://doi.org/10.1038/s41598-022-05364-y.
5. B. Liu, Y. L. Siu, and G. Mitchell, "Hazard interaction analysis for multi-hazard risk assessment: A systematic classification based on hazard-forming environment," *Natural Hazards and Earth System Sciences*, vol. 16, no. 2, pp. 629–642, Mar. 2016. https://doi.org/10.5194/nhess-16-629-2016.
6. F. E. L. Otto *et al.*, "Climate change increased extreme monsoon rainfall, flooding highly vulnerable communities in Pakistan," *Environmental Research: Climate*, vol. 2, no. 2, p. 025001, Jun. 2023. https://doi.org/10.1088/2752-5295/acbfd5.
7. M. S. Kappes, M. Keiler, K. von Elverfeldt, and T. Glade, "Challenges of analyzing multi-hazard risk: A review," *Natural Hazards*, vol. 64, no. 2, pp. 1925–1958, Oct. 2012. https://doi.org/10.1007/s11069-012-0294-2.
8. A. Dunant, "Are We Missing the Target? A Bias-Variance Perspective on Multi-Hazard Risk Assessment," *Front Earth Sci (Lausanne)*, vol. 9, May 2021. https://doi.org/10.3389/feart.2021.685301.
9. Syamsidik *et al.*, "Fifteen years of the 2004 Indian Ocean Tsunami in Aceh-Indonesia: Mitigation, preparedness and challenges for a long-term disaster recovery process," *International Journal of Disaster Risk Reduction*, vol. 54, no. November 2020, p. 102052, 2021. https://doi.org/10.1016/j.ijdrr.2021.102052.
10. A. Tilloy, B. D. Malamud, H. Winter, and A. Joly-Laugel, "A review of quantification methodologies for multi-hazard interrelationships," *Earth Sci Rev*, vol. 196, no. June, p. 102881, 2019. https://doi.org/10.1016/j.earscirev.2019.102881.
11. Scopus, "Documents titled {Systemic Risk} - Analyze search results of 1761 documents," May 2024.
12. M. Mycoo *et al.*, "Small islands," in *In Climate Change*, vol. 15, Springer Netherlands, 2022, pp. 2043–2121. https://doi.org/10.1017/9781009325844.017.

13. A. R. Gusman, J. Roger, C. Noble, X. Wang, W. Power, and D. Burbidge, "The 2022 Hunga Tonga-Hunga Ha'apai Volcano Air-Wave Generated Tsunami," *Pure Appl Geophys*, vol. 179, no. 10, pp. 3511–3525, Oct. 2022. https://doi.org/10.1007/s00024-022-03154-1.
14. S. ann Robinson, "A commentary on national adaptation drivers: The case of small island developing states," *Clim Change*, vol. 154, no. 3–4, pp. 303–313, 2019. https://doi.org/10.1007/s10584-019-02421-w.
15. D. D. P. Thompson, "Compounding challenges for disaster resilience in small island developing states," *Disaster Prevention and Resilience*, pp. 1–20, 2022. https://doi.org/10.20517/dpr.2021.04.
16. M. A. D. Abenir, L. I. O. Manzanero, and V. Bollettino, "Community-based leadership in disaster resilience: The case of small island community in Hagonoy, Bulacan, Philippines," *International Journal of Disaster Risk Reduction*, vol. 71, Mar. 2022. https://doi.org/10.1016/j.ijdrr.2022.102797.
17. Badan Pusat Statistik, *Kota Ternate Dalam Angka 2024*. Kota Ternate, 2024. Accessed: Jan. 26, 2024. [Online]. Available: https://ternatekota.bps.go.id/publication/download.html?.
18. S. Alikaei, M. Rahmani, F. Jamalabadi, M. E. Akdogan, and S. Khoshnevis, "Multi-hazard based land use planning in isolated area; learning from the experience of Pul-e-Khumri City, Afghanistan," *Sustain Cities Soc*, vol. 99, Dec. 2023. https://doi.org/10.1016/j.scs.2023.104873.
19. UNISDR, "Words into Action Guidelines: National Disaster Risk Assessment (Governance System, Methodologies, and Use of Results)," 2017. [Online]. Available: https://www.unisdr.org/files/globalplatform/591f213cf2fbe52828_wordsintoactionguideline.nationaldi.pdf.
20. OpenAI, "Response to query about multi-hazard disaster risk. Retrieved from https://chat.openai.com/chatgpt on 22/05/2024.".
21. M. Ravankhah, M. Schmidt, and T. Will, "Multi-hazard disaster risk identification for World Cultural Heritage sites in seismic zones," *Journal of Cultural Heritage Management and Sustainable Development*, vol. 7, no. 3, pp. 272–289, Sep. 2017. https://doi.org/10.1108/JCHMSD-09-2015-0032.
22. S. Terzi, S. Torresan, S. Schneiderbauer, A. Critto, M. Zebisch, and A. Marcomini, "Multi-risk assessment in mountain regions: A review of modelling approaches for climate change adaptation," *Journal of Environmental Management*, vol. 232. Academic Press, pp. 759–771, Feb. 15, 2019. https://doi.org/10.1016/j.jenvman.2018.11.100.
23. Z. Liu, F. Nadim, A. Garcia-Aristizabal, A. Mignan, K. Fleming, and B. Q. Luna, "A three-level framework for multi-risk assessment," *Georisk*, vol. 9, no. 2, pp. 59–74, Apr. 2015. https://doi.org/10.1080/17499518.2015.1041989.
24. J. C. Gill and B. D. Malamud, "Reviewing and visualizing the interactions of natural hazards," *Reviews of Geophysics*, vol. 52, no. 4. Blackwell Publishing Ltd, pp. 680–722, 2014. https://doi.org/10.1002/2013RG000445.
25. C. J. van Westen and S. Greiving, "Multi-hazard risk assessment and decision making," in *Environmental Hazards Methodologies for Risk Assessment and Management*, 1st ed., vol. 1, N. R. Dalezios, Ed., London: IWA Publishing, 2017, pp. 31–91.
26. W. Marzocchi, A. Garcia-Aristizabal, P. Gasparini, M. L. Mastellone, and A. Di Ruocco, "Basic principles of multi-risk assessment: A case study in Italy," *Natural Hazards*, vol. 62, no. 2, pp. 551–573, Jun. 2012. https://doi.org/10.1007/s11069-012-0092-x.
27. P. Nejedlik and N. R. Dalezios, "Hazards information management and services," in *Environmental Hazards Methodologies for Risk Assessment and Management*, Nicolas R. Dalezios., IWA Publishing, 2017, pp. 503–527.
28. U. Barua, M. S. Akhter, and M. A. Ansary, "District-wise multi-hazard zoning of Bangladesh," *Natural Hazards*, vol. 82, no. 3, pp. 1895–1918, Jul. 2016. https://doi.org/10.1007/s11069-016-2276-2.
29. W. M. Abdulwahid and B. Pradhan, "Landslide vulnerability and risk assessment for multi-hazard scenarios using airborne laser scanning data (LiDAR)," *Landslides*, vol. 14, no. 3, pp. 1057–1076, Jun. 2017. https://doi.org/10.1007/s10346-016-0744-0.
30. S. K. Aksha, L. M. Resler, L. Juran, and L. W. Carstensen, "A geospatial analysis of multi-hazard risk in Dharan, Nepal," *Geomatics, Natural Hazards and Risk*, vol. 11, no. 1, pp. 88–111, Jan. 2020. https://doi.org/10.1080/19475705.2019.1710580.
31. A. Carpignano, E. Golia, C. Di Mauro, S. Bouchon, and J. P. Nordvik, "A methodological approach for the definition of multi-risk maps at regional level: First application," *J Risk Res*, vol. 12, no. 3–4, pp. 513–534, Apr. 2009. https://doi.org/10.1080/13669870903050269.
32. A. Triyanti *et al.*, "Governing systemic and cascading disaster risk in Indonesia: Where do we stand and future outlook," *Disaster Prevention and Management: An International Journal*, vol. 32, no. 1, pp. 27–48, Jun. 2023. https://doi.org/10.1108/DPM-07-2022-0156.
33. R. Jati, Udrekh, S. E. Purba, O. Shalih, A. Adi, and et.al., "Risiko Bencana Indonesia 'Memahami Risiko Sistemik di Indonesia,'" 2023. Accessed: May 28, 2023. [Online]. Available: https://inarisk.bnpb.go.id/BUKU-RBI-2022/mobile/index.html#p=1.

34. S. Greiving, M. Fleischhauer, and J. Lückenkötter, "A methodology for an integrated risk assessment of spatially relevant hazards," *Journal of Environmental Planning and Management*, vol. 49, no. 1, pp. 1–19, Jan. 2006. https://doi.org/10.1080/09640560500372800.
35. Y. Depietri, K. Dahal, and T. McPhearson, "Multi-hazard risks in New York City," *Natural Hazards and Earth System Sciences*, vol. 18, no. 12, pp. 3363–3381, Dec. 2018. https://doi.org/10.5194/nhess-18-3363-2018.
36. S. B. Ajjur and Y. K. Mogheir, "Flood hazard mapping using a multi-criteria decision analysis and GIS (case study Gaza Governorate, Palestine)," *Arabian Journal of Geosciences*, vol. 13, no. 2, Jan. 2020. https://doi.org/10.1007/s12517-019-5024-6.
37. T. De Pippo, C. Donadio, M. Pennetta, C. Petrosino, F. Terlizzi, and A. Valente, "Coastal hazard assessment and mapping in Northern Campania, Italy," *Geomorphology*, vol. 97, no. 3–4, pp. 451–466, May 2008. https://doi.org/10.1016/j.geomorph.2007.08.015.
38. C. van Westen, M. S. Kappes, B. Q. Luna, S. Frigerio, T. Glade, and J. P. Malet, "Medium-scale multi-hazard risk assessment of gravitational processes," in *Advances in Natural and Technological Hazards Research*, vol. 34, Springer Netherlands, 2014, pp. 201–231. https://doi.org/10.1007/978-94-007-6769-0_7.
39. B. W. Mutaqin, W. Handayani, F. Satya Candra Rosaji, D. Wahyuningtyas, and M. Aris Marfai, "GEOMORPHOLOGICAL ANALYSIS FOR THE IDENTIFICATION OF SMALL VOLCANIC ISLANDS IN NORTH MALUKU, INDONESIA," *Jurnal Geografi*, vol. 13, no. 2, pp. 184–194, 2021, [Online]. Available: http://jurnal.unimed.ac.id/2012/index.php/geo.
40. B. W. Mutaqin *et al.*, "Geomorphology of the small island of Tidore and Hiri (North Maluku, Indonesia)," in *E3S Web of Conferences*, EDP Sciences, 2021, p. 03012. https://doi.org/10.1051/e3sconf/202132503012.
41. F. Firmansyah, "Identifikasi Tingkat Risiko Bencana Letusan Gunung Api Gamalama di Kota Ternate," *Jurnal Lingkungan dan Bencana Geologi*, vol. 2, no. 3, pp. 203–219, 2011.
42. N. Nagu, M. R. Lessy, and R. Achmad, "Adaptation Strategy of Climate Change Impact on Water Resources in Small Island Coastal Areas: Case Study on Ternate Island-North Maluku," *KnE Social Sciences*, vol. 3, no. 5, p. 424, 2018. https://doi.org/10.18502/kss.v3i5.2347.
43. Ikqra, B. Tjahjono, and E. Sunarti, "Studi Geomorfologi Pulau ternate dan Penilaian Bahaya Longsor," *Jurnal Tanah Lingkungan*, vol. 14, no. 1, pp. 1–6, 2012. https://doi.org/10.29244/jitl.14.1.1-6.
44. A. Hidayat, M. A. Marfai, and D. S. Hadmoko, "Eruption hazard and challenges of volcanic crisis management on a small Island: A case study on Ternate Island - Indonesia," *International Journal of GEOMATE*, vol. 18, no. 66, pp. 171–178, 2020. https://doi.org/10.21660/2020.66.ICGeo43.
45. Badan Nasional Penanggulangan Bencana (BNPB), "Dokumen Kajian Risiko Bencana Kota Ternate, Provinsi Maluku Utara," Badan Nasional Peanggulangan Bencana, 2012.
46. K. Evrita, M. A. Marfai, N. Khakim, and E. T. W. Mei, "Tsunami susceptibility mapping in the coastal area of Ternate Island," in *Proc. SPIE 11372, Sixth International Symposium on LAPAN-IPB Satellite*, 2014.
47. S. Sabaruddin and R. Rasyid, "Utilization of QGIS 3.22 with a Spatial Approach in Assessing Tsunami Risk on Small Islands in Ternate City," *Techno Jurnal Penelitian*, vol. 12, no. 2, Oct. 2023. https://doi.org/10.33387/tjp.v12i2.6771.
48. A. M. Angkotasan, I. W. Nurjaya, and N. M. N. Natih, "Analisis Perubahan Garis Pantai Di Pantai Barat Daya Pulau Ternate , Provinsi Maluku Utara (Shoreline Change Analysis of the South West Coast At Ternate Island , North Molucas Province)," *Jurnal Teknologi Perikanan dan Kelautan*, vol. 3, no. 1, pp. 11–22, 2012. https://doi.org/10.24319/jtpk.3.11-22.
49. M. R. Lessy and R. M. Abdullah, "Forecasting of Significant Wave Height and Period at Western Waters of Ternate Island, North Maluku," *Techno: Jurnal Penelitian*, vol. 10, no. 1, 2021. https://doi.org/10.33387/tjp.v10i1.3026.
50. A. Sofyan, Dudibiyakto, and L. Sahubawa, "Kajian Erosi Marine Sebagai Penyebab Degradasi Kepesisiran Kota Ternate," *Jurnal Manusia dan Lingkungan*, vol. 17, no. 2, pp. 89–97, 2010. https://doi.org/10.22146/jml.18707.
51. A. Hidayat, M. A. Marfai, and D. S. Hadmoko, "Eruption on Indonesia's volcanic islands: A review of potential hazards, fatalities, and management," in *IOP Conference Series: Earth and Environmental Science*, 2020, pp. 0–11. https://doi.org/10.1088/1755-1315/485/1/012061.
52. Ikqra, "Analisis bentuk lahan (Landform) untuk penilaian bahaya longsor di Pulau Ternate Provinsi Maluku Utara," *Dialog Penanggulangan Bencana*, vol. 4, no. 2, p. . 35-46, 2013.
53. C. Sulaeman and A. Cipta, "Model intensitas gempa bumi di Maluku Utara Earthquake Intensity Model in North Maluku," *Jurnal Lingkungan dan Bencana Geologi*, vol. 3, no. 2, pp. 79–88, 2012. https://doi.org/10.34126/jlbg.v3i2.38.
54. Nasarudin, S. Rahedin, and K. Suliamin, "Analisis Kesiapsiagaan Masyarakat Pada Wilayah Rawan Banjir Lahar Dingin Gunung Gamalama Kelurahan Dufa-Dufa Ternate," *Jurnal Spasial*, vol. 6, no. 2, pp. 54–62, 2019. https://doi.org/10.22202/js.v6i2.3735.
55. M. R. Lessy, A. K. Arif, F. Marassabessy, R. Wahyuningrum, and N. Nagu, "Kapasitas Adaptif Masyarakat di Wilayah Pesisir Terhadap Bencana (Studi Kasus Bencana Banjir di Kelurahan Bastiong Karance Kota Terante)," in *Prosiding Seminar Nasional Kemaritiman dan Sumberdaya Pulau-Pulau Kecil*, 2017, pp. 77–85.

56. A. Y. Priambodo and M. Kamis, "Delineasi DAS sungai penyebab banjir di Kelurahan Rua Kecamatan Pulau Ternate Kota Ternate menggunakan HEC-HMS," *Jurnal SIPILsains*, vol. 10, no. 2, 2020, Accessed: May 26, 2021. [Online]. Available: https://ejournal.unkhair.ac.id/index.php/sipils/article/view/151-156.
57. J. Rasai, D. Muslim, N. Sulaksana, and D. Setiadi, "Korelasi Air Limpasan Dengan Perubahan Sungai Tugurara Sebagai Ancaman Bencana Di Kota Ternate Provinsi Maluku Utara," *Jurnal Dialog Penanggulangan Bencana*, vol. 8, no. 2, pp. 120–131, 2017.
58. V. Sabrina, M. Adib Azka, P. Aditya Sugianto, and S, "Kajian Meteorologis saat kejadian bencana Hidrometeorologis di Maluku Utara (Studi kasus: 15-16 Januari 2021," *Jurnal Widya Climago*, vol. 3, no. 2, p. 53, 2021, Accessed: May 28, 2023. [Online]. Available: https://ejournal-pusdiklat.bmkg.go.id/index.php/climago/article/view/35/30.
59. R. M. Said, "Kota Ternate pada masa pemeruntahan Belanda," *Jurnal Penelitian Humano*, vol. 10, no. 2, pp. 426–436, 2019, [Online]. Available: http://ejournal.unkhair.ac.id/index.php/humano.
60. H. A. Umanailo, P. J. C. Franklin, and J. O. Waani, "Perkembangan Pusat Kota Ternate (Studi Kasus: Kecamatan Ternate Tengah)," *Spasial*, vol. 4, no. 3, pp. 222–233, 2017. https://doi.org/10.35793/sp.v4i3.18268.
61. S. Kosuma, S. W. Palar, and A. L. Ch. P. Lapian, "Analisis Struktur Perekonomian Dan Pertumbuhan Ekonomi Di Kota Ternate," *Jurnal Berkala Ilmiah Efisiensi*, vol. 16, no. 2, pp. 507–516, 2016, Accessed: May 28, 2023. [Online]. Available: https://ejournal.unsrat.ac.id/v3/index.php/jbie/article/view/12757/12350.
62. H. Saputra, A. Wahid Hasyim, and A. Rachmansyah, "Penataan Kawasan Bencana Lahar Dingin Di Kecamatan Ternate Tengah Dan Ternate Utara," *Indonesian Green Technology Journal*, vol. 4, no. 1, pp. 1–10, 2015, [Online]. Available: https://igtj.ub.ac.id/index.php/igtj/article/view/130.
63. A. Hidayat, M. A. Marfai, and D. S. Hadmoko, "The 2015 eruption of Gamalama volcano (Ternate Island–Indonesia): Precursor, crisis management, and community response," *GeoJournal*, Feb. 2020. https://doi.org/10.1007/s10708-020-10237-w.
64. A. G. Pradiptasari, J. O. Waani, and W. Mononimbar, "Sistem Penanggulangan Bencana Gunung Api Gamalama di Permukiman Kampung Tubo Kota Ternate," *Spasial: Perencanaan Wilayah dan Kota*, vol. 2, no. 3, pp. 33–42, 2015. https://doi.org/10.35793/sp.v2i3.9828.
65. Supartoyo, "Gempa Bumi Laut Maluku Tanggal 15 November 2014," *Jurnal Lingkungan dan Bencana Geologi*, vol. 6, no. 1, pp. 45–58, 2015. https://doi.org/10.34126/jlbg.v6i1.75.
66. M. Brilliantina, H. Pratiwi, and Y. Susanti, "Analisis Seismisitas pada Data Gempa Bumi di Provinsi Maluku Utara Penerapan Model Epidemic Type Aftershock Sequence (ETAS)," *Prosiding Pendidikan Matematika dan Matematika*, vol. 4, 2021.
67. A. Saifuddin and E. I. Pertiwi, "Pemetaan Zona Risiko Gempabumi berdasarkan Peak Ground Acceleration Terhadap Energi dan Sumberdaya Mineral di Provinsi Maluku Utara," *Seminar Nasional Geomatika*, p. 171, Apr. 2021. https://doi.org/10.24895/sng.2020.0-0.1132.
68. L. Hamzah, N. T. Puspito, and F. Imamura, "Tsunami Catalog and Zones in Indonesia.," *Journal of Natural Disaster Science*, vol. 22, no. 1, pp. 25–43, 2000. https://doi.org/10.2328/jnds.22.25.
69. Yudhicara and Syahrir Lukman, "Temuan Endapan Paleotsunami di Pulau Ternate: Bersiap untuk Selamat," *Jurnal Geologi dan Sumberdaya Mineral*, vol. 25, no. 1, pp. 41–53, Feb. 2024. https://doi.org/10.33332/jgsm.geologi.v25i1.770.
70. A. R. Gusman, A. D. Nugraha, and H. A. Shiddiqia, "Hypocenter relocations and tsunami simulation for the 15 November 2014 Northern Molucca Sea earthquake in Indonesia," *Jurnal Geofisika*, vol. 15, no. 01, 2017, [Online]. Available: https://inatews.bmkg.go.id/new/view.
71. A. La Masinu, M. Riva, and D. La Mane, "Fenomena Gunung Api Gamalama Terhadap Dampak Aliran Lahar," *Jurnal Pendidikan Geografi*, vol. 23, no. 2, pp. 113–121, Jun. 2018. https://doi.org/10.17977/um017v23i22018p113.
72. C. Bonadonna *et al.*, "Integrating hazard, exposure, vulnerability and resilience for risk and emergency management in a volcanic context: The ADVISE model," *Journal of Applied Volcanology*, vol. 10, no. 1, Dec. 2021. https://doi.org/10.1186/s13617-021-00108-5.
73. E. Aldrian and R. Dwi Susanto, "Identification of three dominant rainfall regions within Indonesia and their relationship to sea surface temperature," *International Journal of Climatology*, vol. 23, no. 12, pp. 1435–1452, 2003. https://doi.org/10.1002/joc.950.
74. A. Y. Elake, M. Talahatu, and P. Nanlohy, "Korelasi Multivariabel Enso, Monsun Dan Dipolemode Terhadap Variabilitas Curah Hujan Di Maluku," *Barekeng: Jurnal Ilmu Matematika Dan Terapan*, vol. 12, no. 1, p. 7, 2018. https://doi.org/10.30598/vol12iss1pp7-16ar359.
75. A. F. Girma, "Analyzing Open Source, Phyton-Based, tools for Multi-hazard Risk Assessment," Thesis, University of Twente, Enschede, 2021. Accessed: Feb. 15, 2022. [Online]. Available: https://essay.utwente.nl/88723/.
76. H. Kurnio, T. Naibaho, and C. Purwanto, "Review of Submarine Landslides in the Eastern Indonesia Region," *Bulletin of the Marine Geology*, vol. 34, no. 2, pp. 63–76, 2019.

77. K. D. Buck and J. K. Summers, "Application of a multi-hazard risk assessment for local planning," *Geomatics, Natural Hazards and Risk*, vol. 11, no. 1, pp. 2058–2078, Jan. 2020. https://doi.org/10.1080/19475705.2020.1828190.
78. Y. R. Sarihi, S. Tilaar, and M. M. Rengkung, "Analisis Penggunaan lahan di Pulau Ternate," *Jurnal SPASIAL*, vol. 7, no. 3, 2020, Accessed: May 26, 2022. [Online]. Available: https://ejournal.unsrat.ac.id/v3/index.php/spasial/article/view/30840.
79. A. T. Vrita, R. Salam, and A. Farida, "Prediksi Kebutuhan Area Permukiman di Kota Ternate," *Space*, vol. 8, pp. 111–122, 2021.
80. P. C. Latue, "Analisis Spasial Temporal Perubahan Tutupan Lahan di Pulau Ternate Provinsi Maluku Utara Citra Satelit Resolusi Tinggi," *Buana Jurnal Geografi, Ekologi dan Kebencanaan*, vol. 1, no. 1, pp. 31–38, Aug. 2023. https://doi.org/10.56211/buana.v1i1.339.
81. BPBD Kota Ternate, "Data Kejadian Kencana Kota Ternate 2020-2021 ," Ternate, Jan. 2021.
82. V. Sabrina, M. A. Azka, and P. A. Sugianto, "Kajian meteorologis saat kejadian bencana hidrometeorologis di Maluku Utara," *Jurnal Widya Climago*, vol. 3, no. 2, pp. 53–60, 2021.
83. A. Sofyan, Sunarto, Sudibiyakto, and L. Sahubawa, "The Study of Marine Erosion as a Coastal degradation in Ternate City," *Jurnal Manusia dan Lingkungan*, vol. 17, no. 2, pp. 89–97, 2010. https://doi.org/10.22146/jml.18707.
84. E. Tyas Wulan Mei, D. Mardianto, E. Pamudianti, and D. Yanti Amalia, "Physical Assessment of Barangka Tugurara Towards Volcanic Hazards of Gamalama Volcano," 2017.
85. F. Marasabessy, "Hirarki Wilayah Kota Ternate Pasca Pengembangan Kawasan Waterfront City," *Jurnal Wilayah dan Lingkungan*, vol. 4, no. 3, p. 213, 2016. https://doi.org/10.14710/jwl.4.3.213-224.
86. M. Said, "Reklamasi dan Dampaknya Terhadap Wilayah Pesisir Pantai Toboko, Kota Ternate," *Jurnal Dintek*, vol. 12, no. 2, pp. 83–91, 2019.